

Domain Adaptation for Industrial Time-series Forecasting via Causal Inference

Chao Min, Guoquan Wen, Jiangru Yuan, Jun Yi, Xing

Guo

Abstract—Industrial time-series, as a structural data responds to production process information, can be utilized to perform data-driven decision-making for effective monitoring of industrial production process. However, there are some challenges for time-series forecasting in industry, including training cold-start and predicting few-shot caused by data shortage, and decision-confusing caused by unknown causal effect of stochastically treatment policy. To cope with the aforementioned problems, we propose a novel causal domain adaptation framework, Causal Domain Adaptation (CDA) forecaster, for industrial processes. CDA leverages a Conditional Average Treatment Effect (CATE) from sufficiently historical time-series along with treatment policy (source) to improve the performance on the interested domain with limited data (target). In particular, historical data consists of treatments (production measure), covariate (features) and outcome. Firstly, we analyse the causality existing in industrial time-series along with treatments, and thus ensure the shared causality over time. Subsequently, we propose an answer-based attention mechanism to achieve domain-invariant representation by the shared causality in both domains. Then, a novel domain-adaptation method is built to model the treatments and outcomes jointly training on source and target domain. The main insights are that our designed answer-based attention mechanism allows the target domain to leverage the causality existing in source time-series even with different treatments, and our forecaster can predict the counterfactual outcome of industrial time-series after an treatment, meaning a guidance in production process. Compared with commonly baselines, our method on real-world and synthetic oilfield datasets demonstrates the effectiveness in across-domain prediction and the practicality in guiding production process.

Index Terms—Causal inference, Domain adaptation, Industrial time-series, Treatment policy

I. INTRODUCTION

INDUSTRIAL time-series forecasting, as a task reflecting industrial producing process over time, has drawn more attention along with the development of artificial intelligence, where CNN and RNN [1]–[3] are commonly used in forecasting due to their powerful ability in feature representation. There are various deformations of neural networks successfully applied to industry and engineering [4], e.g., mechanical system [5], petroleum industry [6] organic chemistry [7] and biology [8]. In particularly, attention-based transformer-like models [9] have achieved state-of-the-art performance. A downside to these sophisticated models is their reliance on the large dataset with homogeneous time-series for training neural networks [10],

yet collecting and annotating the sufficient data are sometimes expensive and even prohibitive in industrial field. This data-efficiency challenge heavily impedes the adoption of deep learning to a wide spectrum of industry [11].

An effective solution to this challenge is to explore the transferability in deep learning. The transferability extracts transferable representations from source tasks and then adapt it to improve the learning performance for target task [12], [13]. However, once trained, the deep learning models may not generalize well to a new domain of exogenous data since domain shift, that is, the distribution discrepancy between source and target domain [14]. To solve the domain shift issue in deep learning [15], domain adaptation has been proposed to transfer the knowledge of source domain with sufficient data to the target domain with unlabeled or insufficiently labeled data for various tasks. Domain adaptation attempts to capture domain-invariant representations from raw data by aligning features across source and target domains [16]. In their seminal works, domain adaptation method based on neural network, e.g., DANN [17], MMDA [18] is a popular methodology in exploring transferability [19]. In the light of success in time-series task, the related works [20], [21] capture the domain-invariance by confusing the domain discriminator, and then perform the adversarial training. These mechanism ensure they can effectively distinguish representations from different domains, and outperform the metric-based neural network and domain adaptation method in forecasting task [22].

In particular, industrial time-series (outcomes) always change over time and policy (treatments), where treatments is a direct cause for outcomes. In oil and gas industry, for example, gas production is positively affected by treatments such as injection and padding measure [23], [24]. When the sequences of outcomes and treatments are recorded as a time-series, a policy dominates what treatment to take and when for production activity, e.g., improving production and cutting down on accidents. These methods accommodate the sequential causality of industrial time-series in anomaly detection [25]–[27] and outcome prediction [28], [29]. However, they do not directly reveal the latent causality existing in domain shift across the observed distribution of treatments and outcomes [30]. Since the policy itself is generally recorded in industrial production process, we want to infer a causal model of recurrent treatments from sequential treatment-outcome data by utilizing domain adaptation and causal inference [31], [32]. In causal model, there are some consequences should be assessed for industrial production process, including, What

is the causal effect of a given policy? What will be the effect of a change to the treatment policy? What would be happen if the production process had followed a different treatment policy? These questions correspond to observational, interventional, and counterfactual queries. Answering them is crucial, especially in time-series forecasting along with domain shift, as well as a policy decision. Specifically, answering the interventional and counterfactual queries requires modeling policy intervention based on counterfactual inference, while answering the observational query requires time-series forecaster.

Moreover, industrial time-series forecasting under limited data is a typical few-shot problem [33], [34], which can result in poor-forecasting. Few-shot forecasting occurs when there is limited historical matching information in source domain. We can see that these problems are common phenomenon in industrial field due to the expensive cost in collecting and annotating data.

Based on above observations, we can know the advancement of industrial time-series forecasting is challenged by several critical bottlenecks, including

- **Difficulty in collecting and annotating the sufficient data for training.** In industrial producing process, collecting and annotating the sufficient time-series data for training model are expensive and even prohibitive due to complex work conditions or privacy agreement. The data scarcity difficulty will lead to the few-shot problems in domain adaptation.
- **Lack of causal guarantee for time-series forecasting.** While there are fruitful theoretical analyses for industrial time-series forecasting, similar analyses meet substantial hurdles to be extended to causality existing in industrial time-series with treatment policy. Its latent causality can provide the intrinsic relationship among multiple and multivariate time-series. Therefore, it is essential to achieve causal guarantee, which is beneficial to improve forecasting performance and provide producing guidance.
- **Difficulty in charactering the domain-invariant from the causality.** Charactering the domain-invariant involving domain shift requires the built model is time-sensitive in industrial time-series. An effective way is to make the attention mechanism as an encoder, aiming at constructing the domain-invariant representations over time. However, the traditional attention mechanism reconstructs the representation by utilizing the correlation not the causality, resulting in the absence of causality in domain shift. Thus, it leads to a difficulty in estimating the causal impact of policy.

To figure out these situations, we propose a causal domain adaptation (CDA) framework, a novel sequence-to-sequence forecaster for industrial time-series forecasting. CDA leverages the advances in domain adversarial training and causal inference to construct a industrial time-series forecaster, which attempts to perform causal modeling across treatment-outcome and policy sequence. Our main contributions are as follows,

- **Treatment-invariant representations over time.** Distinct from attention mechanism, CDA utilizes counter-

factual inference to construct the domain-invariant representations over time, i.e., treatment-invariant information which can break the association between history-matching and treatment alignment of time-series. Thus, the latent causality ensure that even limited data can provide the sufficient temporal information for time-series modeling. For this, domain adversarial training is employed to trade-off between the treatment-invariant representations and time-series forecasting. We show that the representations remove the bias caused by policy and can be reliably used for forecasting industrial time-series. This contribution also provides the causal guarantee for time-series forecasting from the treatment policy.

- **Counterfactual estimation for future producing activity.** To estimate counterfactual outcome for treatment policy, we integrate an average causal effect estimation (CATE) as a part of a sequence-to-sequence architecture. CATE is mainly utilized to perform the causal domain-invariant representation and calculate the causal effect of treatment policy impacting on outcome sequence. Thus, CDA can answer the question, which policy is most effective for producing activity? We illustrate in Fig.?? the applicability of CDA in counterfactual estimation and optimizing in oil and gas filed.

In our experiments, we evaluate CDA in the realistic datasets with treatment policy in oil and gas field. We show that CDA achieves better performance in forecasting monthly oil production, but also in choosing the optimal treatment policy in improving oil production.

II. PRELIMINARIES

Our work mainly builds on causal inference and domain adaptation.

A. Casual Inference

Casual inference is the process of drawing a conclusion about a causal connection based on the conditions of the occurrence of an effect [31]. It is well known that “correlation does not imply causation.” The main difference between causality and correlation analysis is that former analyzes the response of the effect variable when the cause is changed. In this section, we briefly introduce causal graph, treatment intervention and counterfactual inference for our method [35]. And we also define a causal answer formally, while using SCM to emphasize the distinction between probability distributions induced by different types of causal answer.

Causal Graph. Let $\mathcal{M} := (\mathbf{S}, p(\epsilon))$ denote a structural causal model (SCM), which consists of structural assignments $\mathbf{S} = \{\mathbf{x}_i := f_i(\epsilon_i; \mathbf{pa}_i)\}_{i=1}^N$ over structural model f and joint distribution $p(\epsilon) = \prod_{i=1}^N p(\epsilon_i)$ over noise variables ϵ . In addition, \mathbf{pa}_i is the set of parents of \mathbf{x}_i (its direct causes). Then, a causal graph \mathcal{G} is obtained by representing each variable \mathbf{x}_i as node and draw edges to \mathbf{x}_i from its parents $\mathbf{pa}(\mathbf{x}_i)$. Formally, time-series $\mathbf{pa}(\mathbf{x}_i)$ is said to be a temporal cause of \mathbf{x}_i when the values of $\mathbf{pa}(\mathbf{x}_i)$ provide statistically significant information about the future values of \mathbf{x}_i .

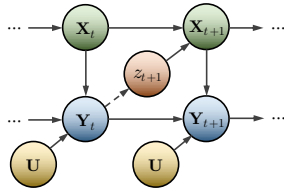


Fig. 1: The causal graph \mathcal{G} in continuous time, where $a \rightarrow b$ means a is the direct cause of b . And the treatment policy z_{t+1} can be specified by human (dashed arrow) or determined by previous outcome Y_t , U denote the static variables.

Treatment Intervention. Let \mathbf{X} , \mathbf{Y} and \mathbf{Z} denote the covariate, outcome, and treatment variable, respectively. In causal inference, $\mathbf{Y}(\mathbf{X}, \mathbf{z}_i)$ is a random variable that represents the value of outcome \mathbf{Y} under a treatment policy \mathbf{z}_i and covariate \mathbf{X} . The treatment intervention on \mathbf{Z} by \mathbf{z}_i corresponds to the *do-operator* $\text{do}(\mathbf{Z} = \mathbf{z}_i)$ in the SCM, as $P(\mathbf{Y}(\mathbf{X}, \mathbf{z}_i)) = P(\mathbf{Y}|\mathbf{X}, \text{do}(\mathbf{Z} = \mathbf{z}_i))$, where $\text{do}(\mathbf{Z} = \mathbf{z}_i)$ means the treatment policy is forced to intervene to \mathbf{z}_i .

Counterfactual Inference. In counterfactual queries, given a history of past events that have already occurred, one asks what past events would have instead occurred if certain intervention had been in place. The counterfactual can be formulized as $P(\mathbf{Y}(\mathbf{X}, \mathbf{z}_i)|\mathbf{X}, \mathbf{z}_j)$, where \mathbf{X}, \mathbf{z}_j corresponds to the past events $\mathbf{Y}(\mathbf{X}, \mathbf{Z} = \mathbf{z}_j)$ and $\mathbf{Y}(\mathbf{X}, \mathbf{z}_i)$ corresponds to a query that if we make an intervention with $\text{do}(\mathbf{Z} = \mathbf{z}_i)$, what will happen to \mathbf{Y} under the trained model f , i.e., past events $\mathbf{Y}(\mathbf{X}, \mathbf{Z} = \mathbf{z}_j)$.

The difference between treatment intervention $P(\mathbf{Y}|\mathbf{X}, \text{do}(\mathbf{Z} = \mathbf{z}_i))$ and counterfactuals inference $P(\mathbf{Y}(\mathbf{X}, \mathbf{z}_i)|\mathbf{X}, \mathbf{z}_j)$ are highlighted by joint-distribution: (i) a treatment intervention requires access to the treatment distribution $\mathbf{z}_i \sim P(\mathbf{Z})$ and only use the noise prior $P(\epsilon)$; (ii) a counterfactual inference requires access to the counterfactual distribution $\mathbf{z}_j \sim P(\mathbf{Z})$ and the posterior distribution of noise $P(\epsilon|\mathbf{X}, \mathbf{z}_i)$, which incorporates the knowledge of what already happened. Upon these knowledge, an example of causal graph in continuous time is shown in Fig.1 by causal inference.

B. Domain Adaptation under Causality

In this section, we follow the definitions and notations of domain adaptation in [36]. Accordingly, a domain \mathcal{D} is composed of a feature space \mathcal{X} with marginal probability distribution $P(\mathbf{X})$ and a task \mathcal{T} with label space \mathcal{Y} with conditional probability distribution $P(\mathbf{Y}|\mathbf{X})$, where \mathbf{X} and \mathbf{Y} are the covariate and target variable. By assuming the source domain $\mathcal{D}^S = \{\mathcal{X}^S, P(\mathbf{X}^S)\}$ with $\mathcal{T}^S = \{\mathcal{Y}^S, P(\mathbf{Y}^S|\mathbf{X}^S)\}$ and target domain $\mathcal{D}^T = \{\mathcal{X}^T, P(\mathbf{X}^T)\}$ with $\mathcal{T}^T = \{\mathcal{Y}^T, P(\mathbf{Y}^T|\mathbf{X}^T)\}$, heterogenous domain adaptation can be stated that when the feature spaces of source and target domain satisfy $P(\mathbf{X}^S) \neq P(\mathbf{X}^T)$ with $\mathcal{X}^S = \mathcal{X}^T$ due to domain shift, the label spaces of source and target domain under conditional probability distribution holds that $P(\mathbf{Y}^S|\mathbf{X}^S) \neq P(\mathbf{Y}^T|\mathbf{X}^T)$ with $\mathcal{Y}^S \neq \mathcal{Y}^T$.

As aforementioned, this paper focuses on the domain adaptation in industrial time-series forecasting under treatment pol-

icy. As shown in Fig.1, distinct from non-intervention mode, the domain shift in intervention mode between feature spaces \mathbf{X}^S and \mathbf{X}^T can be detected its causes, mainly concentrating on the corresponding treatment policy $\mathbf{z}_i, \mathbf{z}_j \in \mathbf{Z}$. These can be defined as follows,

$$\begin{aligned} P(\mathbf{X}^S|\mathbf{Z} = \mathbf{z}_i) &\neq P(\mathbf{X}^T|\mathbf{Z} = \mathbf{z}_j) \\ P(\mathbf{Y}^S|\mathbf{X}^S, \mathbf{Z} = \mathbf{z}_i) &\neq P(\mathbf{Y}^T|\mathbf{X}^T, \mathbf{Z} = \mathbf{z}_j) \end{aligned} \quad (1)$$

where \mathbf{z}_i and \mathbf{z}_j denote the treatment policy in source and target domain, namely the conditions.

Causal structure. Intervened by treatment policy, source and target domains of industrial time-series have different distribution but share the same causal structure over time, shown in the top of Fig.1. Specifically, similar to the aforementioned notation of causal inference, the domain adaptation under causality has the similar probability representation, which can be category into two main groups depending on treatment policy or counterfactual inference. By utilizing cause \mathbf{Z} , namely treatment policy, the bridging theory of domain adaptation for treatment intervention can be defined as $P(\mathbf{X}^S|\mathbf{Z} = \mathbf{z}_i) \neq P(\mathbf{X}^T|\text{do}(\mathbf{Z} = \mathbf{z}_j))$, while for counterfactual inference can be defined as $P(\mathbf{Y}^S|\mathbf{X}^S, \mathbf{Z} = \mathbf{z}_i) \neq P(\mathbf{Y}^T(\mathbf{X}^S, \mathbf{z}_i)|\mathbf{X}^T, \text{do}(\mathbf{Z} = \mathbf{z}_j))$

III. METHOD

In this section, the problem setup and notation used to study treatment-outcome and domain adaptation is introduced. And then the bulit method will be proposed, that is, the causal domain adaptation (CDA).

A. Problem formulation

Considering an observational N time-series dataset $\mathcal{D} = \left\{ \left(\mathbf{x}_t^{(i)}, \mathbf{y}_t^{(i)}, \mathbf{z}_t^{(i)} \right)_{t=1}^{T^{(i)}} \right\}_{i=1}^N$, each observation consists of time-dependent covariates $\mathbf{x}_t^{(i)} \in \mathcal{X}_t$, treatments received from $\mathbf{z}_t^{(i)} \in \{z_1, z_2, \dots, z_K\}$ and outcomes $\mathbf{y}_t^{(i)} \in \mathcal{Y}_t$. for $T^{(i)}$ discrete timesteps. In time-series forecasting, given the history of the covariates $\mathbf{X}_{1:t} = (\mathbf{x}_1, \mathbf{x}_2, \dots, \mathbf{x}_t)$ and treatment assignments $\mathbf{Z}_{1:t} = (\mathbf{z}_1, \mathbf{z}_2, \dots, \mathbf{z}_t)$, we want to make τ predictions of outcomes $\mathbf{Y}_{t+1:t+\tau} = (\mathbf{y}_{t+1}, \mathbf{y}_{t+2}, \dots, \mathbf{y}_{t+\tau})$ via future sequence and time-series generator G ,

$$\mathbf{Y}_{t+1:t+\tau}(\mathbf{X}_{t+1:t+\tau}, \mathbf{Z}_{t+1:t+\tau}) = G(\mathbf{X}_{1:t}, \mathbf{Z}_{1:t}, \mathbf{Y}_{1:t}) \quad (2)$$

According to the Eq.(2), the history of time-series can be used to train a supervised sequence generator by the probability formulation $P(\mathbf{Y}_{t+1:t+\tau}(\mathbf{X}_{t+1:t+\tau}, \mathbf{Z}_{t+1:t+\tau})|\mathbf{X}_{1:t}, \mathbf{Z}_{1:t}, \mathbf{Y}_{1:t})$. Furthermore, in industrial time-series forecasting, the treatment policy $\mathbf{Z}_{t+1:t+\tau}$ can be specified in advance. Then, conditioned on the history $(\mathbf{X}_{1:t}, \mathbf{Z}_{1:t}, \mathbf{Y}_{1:t})$ and shared causality over time, the causal effect of the treatment $\mathbf{Z}_{t+1:t+\tau}$ on the outcome trajectory is fully mediated through sequential covariates $\mathbf{X}_{t+1:t+\tau}$ ([37] Theorem 1.),

$$\begin{aligned} &P(\mathbf{Y}_{t+1:t+\tau}(\mathbf{X}_{t+1:t+\tau}, \mathbf{Z}_{t+1:t+\tau})|\mathbf{X}_{1:t}, \mathbf{Z}_{0:t-1}, \mathbf{Y}_{1:t}) \\ &= P(\mathbf{Y}_{>t}(\mathbf{X}_{>t}, \mathbf{Z}_{>t})|\mathbf{H}_{\leq t}) \\ &= P(\mathbf{Y}_{>t}|\mathbf{H}_{\leq t}, \mathbf{X}_{>t}, \mathbf{Z}_{>t})P(\mathbf{X}_{>t}|\mathbf{H}_{\leq t}, \mathbf{Z}_{>t})P(\mathbf{Z}_{>t}|\mathbf{H}_{\leq t}) \end{aligned} \quad (3)$$

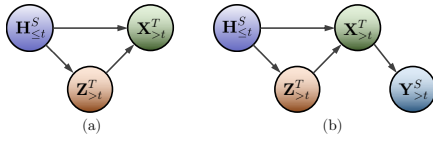


Fig. 2: The shared causality for both both domains in treatment term and outcome term. (a). The causality in treatment-policy term; (b). The causality in outcome term.

where $\mathbf{H}_{\leq t} = [\mathbf{X}_{1:t}, \mathbf{Z}_{1:t}, \mathbf{Y}_{1:t}]$, $\mathbf{X}_{>t} = \mathbf{X}_{t+1:t+\tau}$, $\mathbf{Z}_{>t} = \mathbf{Z}_{t+1:t+\tau}$ and $\mathbf{Y}_{>t} = \mathbf{Y}_{t+1:t+\tau}$. Accordingly, using the time-lag response in industrial time-series, both of which can be estimated with a specified time-series model,

$$\underbrace{P(\mathbf{Y}_{>t}|\mathbf{H}_{\leq t}, \mathbf{X}_{>t}, \mathbf{Z}_{>t})}_{\text{Outcome Term}} \underbrace{P(\mathbf{X}_{>t}|\mathbf{H}_{\leq t}, \mathbf{Z}_{>t})P(\mathbf{Z}_{>t}|\mathbf{H}_{\leq t})}_{\text{Treatment Term}} \quad (4)$$

Apparently, the identifiability result in Eq.(4) generalize the forecasting task to a time-dependent covariate forecasting module, namely **Treatment Term**, and another outcome forecasting module, namely **Outcome Term**.

B. Joint Treatment-Outcome Model

To estimate both statistical terms in Eq.(4), i.e., Treatment Term and Outcome Term, from observational time-series, we propose a joint treatment-outcome model, combining a counterfactual inference process and conditional domain adaptation process.

Shared Causality Module in Treatment Term and Outcome Term. We design a causality module to be shared by both source domain and target domain, since treatment term and outcome term have different distributions but share same causal structure, where the data in treatment term and outcome term with subscript $\leq t$ corresponds to source domain, and the data with subscript $> t$ corresponds to target domain.

For **Treatment Term** in Eq.(4), it consists of two sub-term, i.e., $P(\mathbf{X}_{>t}|\mathbf{H}_{\leq t}, \mathbf{Z}_{>t})$ and $P(\mathbf{Z}_{>t}|\mathbf{H}_{\leq t})$ called treatment-covariate term and treatment-policy term. For treatment-policy term, treatment policy can be artificially specified in advance, thus it is simplified to $\mathbf{Z}_{>t} = \{\mathbf{z}_t\}_{t+1}^{t+\tau}$. For treatment-covariate term in domain adaptation, its different distributions denoted by $P(\mathbf{X}_{>t}^T|\mathbf{H}_{\leq t}^S, \mathbf{Z}_{>t}^T) \neq P(\mathbf{X}_{\leq t}^S)$ since the treatment policy $\mathbf{Z}_{\leq t}^S (\subseteq \mathbf{H}_{\leq t}^S)$ in source domain may be distinct from the treatment policy $\mathbf{Z}_{>t}^T$ in target domain, e.g., human intervention.

For **Outcome Term** in Eq.(4) under domain adaptation, its different distributions denoted by $P(\mathbf{Y}_{>t}^T|\mathbf{H}_{\leq t}^S, \mathbf{X}_{>t}^T, \mathbf{Z}_{>t}^T) \neq P(\mathbf{Y}_{\leq t}^S)$ since $\mathbf{X}_{\leq t}^S$ in source domain is distinct from $\mathbf{X}_{>t}^T$ in target domain caused by the difference between treatment policies \mathbf{Z} .

In industrial time-series forecasting, although there is domain shift existing in treatment term and outcome term, domain-invariant representation can be extracted from causal mechanism perspective between domains. Shown in Fig.2, the domain-invariant causality mean that the intrinsic causality will not change along with time t or domain S, T , including $\mathbf{H}_{\leq t}, \mathbf{Z}_{>t}$ are the direct cause of $\mathbf{X}_{>t}$, while $\mathbf{X}_{>t}$ is the direct cause of $\mathbf{Y}_{>t}$. Under this view, these causality indicates

that treatment policy $\mathbf{Z}_{>t}^T$ is a primary cause for domain drift excluding the history-matching $\mathbf{H}_{\leq t}$. Since we cast the industrial time-series forecasting in terms of a domain adaptation problem, the query of attention mechanism is accessible refer to the treatment policy $\mathbf{Z}_{>t}$. For simplification, the time-varying treatment $\mathbf{Z}_{>t}$ can be seen as the answers of queries $\mathbf{A}_{>t} = \{\mathbf{a}_t\}_{>t}$, recorded as the answer-based attention mechanism.

Definition 1 (Position-wise CATE). Let \mathbf{z}_t be the assigned treatments over in timestep t , then the position-wise CATE is defined as average causal effect of \mathbf{X}_{t+1} under conditions $\mathbf{H}_{\leq t}$ and do-operator $\text{do}(\mathbf{z}_t)$,

$$\text{CATE}(\mathbf{H}_{\leq t}, \mathbf{z}_t) = \mathbb{E}[\mathbf{X}_{t+1}|\mathbf{H}_{\leq t}, \text{do}(\mathbf{z}_t)] - \mathbb{E}[\mathbf{X}_{t+1}|\mathbf{H}_{\leq t}, \mathbf{z}_t] \quad (5)$$

Reconstruction of Treatment Term and Outcome Term.

Considering the causal effect of \mathbf{z}_t impacting on \mathbf{X}_{t+1} , a position-wise CATE (definition 1) is defined by utilizing $\mathbf{H}_{\leq t}$ and can be used to provide the keys \mathbf{k}_{t+1} for attention mechanism,

$$(\mathbf{a}_t, \mathbf{k}_t) = (\mathbf{z}_t, \text{CATE}(\mathbf{H}_{\leq t}, \mathbf{z}_t)) \quad (6)$$

Thus a causal score α , is computed as the normalized alignment between the answer \mathbf{a}_t and keys $\mathbf{k}_{t'}$ at neighborhood positions $t' \in \mathcal{N}(t)$ using an exponential position-wise CATE as kernel $\mathcal{K}(\cdot, \cdot)$.

$$\alpha(\mathbf{a}_t, \mathbf{k}_{t'}) = \frac{\mathcal{K}(\mathbf{a}_t, \mathbf{k}_{t'})}{\sum_{t' \in \mathcal{N}(t)} \mathcal{K}(\mathbf{a}_t, \mathbf{k}_{t'})} \quad (7)$$

where $\mathcal{K}(\mathbf{a}_t, \mathbf{k}_t) = \exp(\mathbf{k}_t, (\mathbf{H}_{\leq t}, \mathbf{a}_t))$ and $\mathcal{K}(\mathbf{a}_t, \mathbf{k}_t) = \exp(\mathbf{k}_t(\mathbf{H}_{\leq t}, \mathbf{a}_t))$.

For **Treatment Term**, based on the attention mechanism, the reconstruction \mathbf{R}_t of \mathbf{X}_t is produced as the value \mathbf{X}_t weighted by causal score $\alpha(\mathbf{a}_t, \mathbf{k}_{t'})$, followed by

$$\mathbf{R}_{t|\mathbf{a}_t} = \alpha(\mathbf{a}_t, \mathbf{k}_{t'})\mathbf{X}_t, t = 1, 2, \dots \quad (8)$$

Shown in Eq.(8), the reconstruction \mathbf{R}_t depend on the answer \mathbf{a}_t , namely, treatment policy \mathbf{z}_t . Thus, by assigned the available weights for reconstructing the covariates \mathbf{X}_t , the domain discrepancy and time-lags caused by treatment policy \mathbf{z}_t can be negligible in industrial time-series forecasting.

Definition 2 (Conditional Markov Model for Sequence Outcomes). The treatment-outcome assigned with treatment policy follows a Conditional Markov Model,

$$P(\mathbf{Y}_{>t}|\mathbf{H}_{\leq t}, \mathbf{X}_{>t}, \mathbf{Z}_{>t}) = \prod_t P(\mathbf{Y}_{t+1}|\mathbf{H}_{\leq t}, \mathbf{X}_{t+1}, \mathbf{Z}_t) \quad (9)$$

For **Outcome Term**, Conditional Markov Model in definition 2 is applied to achieve the reconstruction of the outcome \mathbf{Y}_{t+1} , which is conditional on the observed covariates $\mathbf{H}_{\leq t}$, the latent covariates \mathbf{X}_{t+1} and possible treatment \mathbf{z}_t . Once the reconstruction of treatment term, i.e., \mathbf{R}_t , has been obtained,

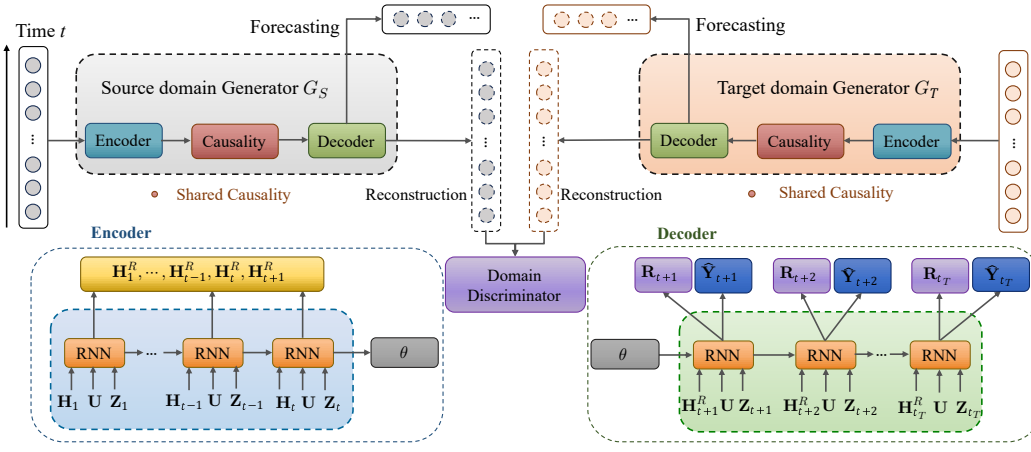


Fig. 3: An architecture overview of CDA forecaster

the reconstruction of outcome term can be generalized via a sequence model [38] with CMM, shown as

$$\mathbb{E}[\mathbf{Y}_{t+1} | \mathbf{H}_{\leq t}^R, \mathbf{R}_{t+1}, \mathbf{Z}_t], t = 1, 2, \dots \quad (10)$$

where $\mathbf{H}_{\leq t}^R = (\mathbf{R}_{1:t}, \mathbf{Z}_{0:t-1}, \mathbf{Y}_{1:t})$ denote the reconstruction of $\mathbf{H}_{\leq t}$.

Once we obtained the reconstruction of treatment term and outcome term, the Eq.(10) is applied to perform domain adaptation via an time-series model, called causal domain adaptation, which aims at time-series forecasting based on answer-based attention mechanism discussed in following subsection.

C. The Causal Domain Adaptation

The proposed method Causal Domain Adaptation (CDA) Forecaster employs a sequence generator to make causal forecasting for industrial time-series. The domain-invariant causality shared by both domains guarantee the effectiveness in reconstructing treatment term and outcome term, while the reconstructions of both terms promote the performance of the learned domain-variant representation in time-series forecasting across domains. Fig.3 illustrates an overview of the proposed architecture.

Adversarial Domain Adaptation. To compute the desired target prediction \mathbf{Y}_t with limited time-series data, the manners of adversarial training on both domains are employed to formulize the following minimax problem,

$$\min_{\mathcal{G}_S, \mathcal{G}_T} \max_B \mathcal{L}_{seq}(\mathcal{D}_S; \mathcal{G}_S) + \mathcal{L}_{seq}(\mathcal{D}_T; \mathcal{G}_T) - \lambda \mathcal{L}_{dom}(\mathcal{D}_S, \mathcal{D}_T; B, \mathcal{G}_S, \mathcal{G}_T) \quad (11)$$

where \mathcal{G}_S and \mathcal{G}_T denote the sequence generators that forecast the sequence for source domain dataset \mathcal{D}_S and target domain dataset \mathcal{D}_T , respectively; parameter $\lambda \geq 0$ balances the estimation error \mathcal{L}_{seq} and domain classification error \mathcal{L}_{dom} , and B denotes a discriminator that classifies the domain between source and target.

Firstly, the loss term $\mathcal{L}_{seq}(\cdot)$ is induced by a sequence

generator G as follows,

$$\mathcal{L}_{seq}(\mathcal{D}; \mathcal{G}) = \sum_{i=1}^N \left(\frac{1}{T} \sum_{t=1}^T l(y_{i,t}^{\mathcal{D}}, y_{i,t}^{\mathcal{G}}) + \frac{1}{\tau} \sum_{t=\tau+1}^{T+\tau} l(y_{i,t}^{\mathcal{D}}, y_{i,t}^{\mathcal{G}}) \right) \quad (12)$$

where $l(\cdot)$ is a loss function and $y_{i,t}^{\mathcal{D}}, y_{i,t}^{\mathcal{G}}$ are the actual sequence and estimated sequence provided by generator \mathcal{G} , respectively.

Definition 3 (Conditional Maximum Mean Discrepancy). Given source \mathcal{S} and target domain \mathcal{T} on the policy space \mathbf{X} and policy condition \mathbf{Z} , leading to the conditional maximum mean discrepancy with reproduction Kernel Hilbert Space \mathcal{H}_k ,

$$d_{\text{CMMD}}(\mathcal{S}|\mathbf{Z}, \mathcal{T}|\mathbf{Z}) = \|\mathbb{E}_{\mathbf{x} \sim \mathcal{S}}[\phi(\mathbf{X}|\mathbf{Z})] - \mathbb{E}_{\mathbf{x} \sim \mathcal{T}}[\phi(\mathbf{X}|\mathbf{Z})]\|_{\mathcal{H}_k} \quad (13)$$

where $\phi(\mathbf{X}|\mathbf{Z}) \in \mathcal{H}$ is feature reconstruction map associated with same condition \mathbf{Z} for source and target domain.

Theorem 1. Let $\mu[P]$ be a distribution of P in RKHS \mathcal{H}_k , then via the reproducing property of RKHS \mathcal{H}_k , we have $\langle \phi, \mu[P_{\mathcal{T}, \mathcal{S}}] \rangle = \mathbb{E}_{\mathbf{x} \sim \mathcal{T}, \mathcal{S}}[\phi(\mathbf{X})]$ for MMD, $\langle \phi, \mu[P_{\mathcal{T}, \mathcal{S}|\mathbf{Z}}] \rangle = \mathbb{E}_{\mathbf{x} \sim \mathcal{T}, \mathcal{S}}[\phi(\mathbf{X}|\mathbf{Z})]$ for CMMD. Thus, the empirical estimate of squared CMMD shown in Definition 3 can be further simplified as

$$\begin{aligned} & d_{\text{CMMD}}^2(\mathcal{S}|\mathbf{Z}, \mathcal{T}|\mathbf{Z}) \\ & \leq \frac{1}{4} [d_{\text{CMMD}}^2(\mathcal{S}|\mathbf{Z}, \mathcal{T}|\mathbf{Z}) + 2d_{\text{CMMD}}(\mathcal{T}, \mathcal{T}|\mathbf{Z})d_{\text{MMD}}(\mathcal{S}, \mathcal{T}) \\ & \quad + d_{\text{CMMD}}^2(\mathcal{S}, \mathcal{S}|\mathbf{Z}) + d_{\text{CMMD}}^2(\mathcal{T}, \mathcal{T}|\mathbf{Z}) + d_{\text{MMD}}^2(\mathcal{S}, \mathcal{T})] \end{aligned}$$

where d_{MMD} is the standard Maximum Mean Distance (MMD), $d_{\text{CMMD}}(\mathcal{S}, \mathcal{S}|\mathbf{Z})$ is applied to measure the closeness of source domain between the raw distributions P_S and condition distribution $P_{S|\mathbf{Z}}$, and $d_{\text{CMMD}}(\mathcal{T}, \mathcal{T}|\mathbf{Z})$ is applied to measure the closeness of target domain between the raw distributions P_T and condition distribution $P_{T|\mathbf{Z}}$.

The proof of Theorem 1 has been presented in Appendix.

Remark 1. The property of CMMD shown in Theorem 1 ensure that CMMD estimate the 4 types of closeness, including conditional closeness between source and target domain, i.e., $d_{\text{CMMD}}(\mathcal{S}|\mathbf{Z}, \mathcal{T}|\mathbf{Z})$, partial conditional closeness between source and target domain, i.e.,

$d_{\text{CMMD}}(\mathcal{S}, \mathcal{S}|\mathbf{Z}), d_{\text{CMMD}}(\mathcal{T}, \mathcal{T}|\mathbf{Z})$ and non-condition loss-ness between source and target domain, i.e., $d_{\text{MMD}}(\mathcal{S}, \mathcal{T})$.

Corollary 1. In domain adversarial learning, the MMD can be transformed into a more tractable form from the perspective of loss function [33], that is,

$$\begin{aligned} d_{\text{CMMD}}^2(\mathcal{S}|\mathbf{Z}, \mathcal{T}|\mathbf{Z}) \\ \Rightarrow \mathcal{L}(\mathcal{D}_{\mathcal{S}}, \mathcal{D}_{\mathcal{T}}, \mathcal{D}_{\mathcal{S}|\mathbf{Z}}, \mathcal{D}_{\mathcal{T}|\mathbf{Z}}; \mathcal{G}_{\mathcal{S}}, \mathcal{G}_{\mathcal{T}}) \\ = \mathcal{L}_1(\mathcal{D}_{\mathcal{S}}, \mathcal{D}_{\mathcal{T}}; \mathcal{G}_{\mathcal{S}}, \mathcal{G}_{\mathcal{T}}) + \mathcal{L}_2(\mathcal{D}_{\mathcal{S}|\mathbf{Z}}, \mathcal{D}_{\mathcal{T}|\mathbf{Z}}; \mathcal{G}_{\mathcal{S}}, \mathcal{G}_{\mathcal{T}}) \quad (14) \\ + \mathcal{L}_3(\mathcal{D}_{\mathcal{S}}, \mathcal{D}_{\mathcal{S}|\mathbf{Z}}; \mathcal{G}_{\mathcal{S}}) + \mathcal{L}_4(\mathcal{D}_{\mathcal{T}}, \mathcal{D}_{\mathcal{T}|\mathbf{Z}}; \mathcal{G}_{\mathcal{T}}) \\ + \mathcal{L}_1(\mathcal{D}_{\mathcal{S}}, \mathcal{D}_{\mathcal{T}}; \mathcal{G}_{\mathcal{S}}, \mathcal{G}_{\mathcal{T}})^{\frac{1}{2}} \mathcal{L}_2(\mathcal{D}_{\mathcal{S}|\mathbf{Z}}, \mathcal{D}_{\mathcal{T}|\mathbf{Z}}; \mathcal{G}_{\mathcal{S}}, \mathcal{G}_{\mathcal{T}})^{\frac{1}{2}} \end{aligned}$$

where $\mathcal{D}_{\mathcal{S}} = \{\mathcal{S}, \hat{\mathcal{S}}\}, \mathcal{D}_{\mathcal{T}} = \{\mathcal{T}, \hat{\mathcal{T}}\}, \mathcal{D}_{\mathcal{S}|\mathbf{Z}} = \{\mathcal{S}, \hat{\mathcal{S}}\}_{|\mathbf{Z}}$ and $\mathcal{D}_{\mathcal{T}|\mathbf{Z}} = \{\mathcal{T}, \hat{\mathcal{T}}\}_{|\mathbf{Z}}$, which $\hat{\mathcal{S}}$ and $\hat{\mathcal{T}}$ denote the generated source and target domains by sequence generators of source domain $\mathcal{G}_{\mathcal{S}}$ and target domain $\mathcal{G}_{\mathcal{T}}$.

$$\begin{cases} \mathcal{L}_1 = \beta_1 \left\| \frac{1}{|\mathcal{D}_{\mathcal{S}}|} \sum_{\mathbf{X} \in \mathcal{D}_{\mathcal{S}}} \mathbf{X} - \frac{1}{|\mathcal{D}_{\mathcal{T}}|} \sum_{\mathbf{X} \in \mathcal{D}_{\mathcal{T}}} \mathbf{X} \right\|_2^2 \\ \mathcal{L}_2 = \beta_2 \left\| \frac{1}{|\mathcal{D}_{\mathcal{S}}|} \sum_{\mathbf{a} \in \mathbf{Z}} \sum_{\mathbf{X} \in \mathcal{D}_{\mathcal{S}|\mathbf{Z}}} \mathbf{R}_{\mathbf{a}} - \frac{1}{|\mathcal{D}_{\mathcal{T}}|} \sum_{\mathbf{a} \in \mathbf{Z}} \sum_{\mathbf{X} \in \mathcal{D}_{\mathcal{T}|\mathbf{Z}}} \mathbf{R}_{\mathbf{a}} \right\|_2^2 \\ \mathcal{L}_3 = \beta_3 \left\| \frac{1}{|\mathcal{D}_{\mathcal{S}}|} \sum_{\mathbf{X} \in \mathcal{D}_{\mathcal{S}}} \mathbf{X} - \frac{1}{|\mathcal{D}_{\mathcal{S}|\mathbf{Z}}|} \sum_{\mathbf{a} \in \mathbf{Z}} \sum_{\mathbf{X} \in \mathcal{D}_{\mathcal{S}|\mathbf{Z}}} \mathbf{R}_{\mathbf{a}} \right\|_2^2 \\ \mathcal{L}_4 = \beta_4 \left\| \frac{1}{|\mathcal{D}_{\mathcal{T}}|} \sum_{\mathbf{X} \in \mathcal{D}_{\mathcal{T}}} \mathbf{X} - \frac{1}{|\mathcal{D}_{\mathcal{T}|\mathbf{Z}}|} \sum_{\mathbf{a} \in \mathbf{Z}} \sum_{\mathbf{X} \in \mathcal{D}_{\mathcal{T}|\mathbf{Z}}} \mathbf{R}_{\mathbf{a}} \right\|_2^2 \end{cases} \quad (15)$$

where $\mathbf{R}_{\mathbf{a}} := \alpha(\mathbf{a}, \mathbf{k})\mathbf{X}$, \mathbf{k} denote the keys in transfer learning, $|\cdot|$ is the cardinality function. and the constants β are the balance parameters.

The proof of Corollary 1 has been presented in Appendix.

Remark 2. The unified loss function $\mathcal{L}(\mathcal{D}_{\mathcal{S}}, \mathcal{D}_{\mathcal{T}}, \mathcal{D}_{\mathcal{S}|\mathbf{Z}}, \mathcal{D}_{\mathcal{T}|\mathbf{Z}}; \mathcal{G}_{\mathcal{S}}, \mathcal{G}_{\mathcal{T}})$ in Corollary 1 consists of 4 types independent loss function, $\mathcal{L}_1, \mathcal{L}_2, \mathcal{L}_3$ and \mathcal{L}_4 . The \mathcal{L}_1 estimate the error between source and target domain, the \mathcal{L}_2 estimate the error between source and target domain with policy, the \mathcal{L}_3 estimate the error between source domain with policy and source domain without policy, the \mathcal{L}_4 estimate the error between target domain with policy and target domain without policy. Thus, $\mathcal{L}(\mathcal{D}_{\mathcal{S}}, \mathcal{D}_{\mathcal{T}}, \mathcal{D}_{\mathcal{S}|\mathbf{Z}}, \mathcal{D}_{\mathcal{T}|\mathbf{Z}}; \mathcal{G}_{\mathcal{S}}, \mathcal{G}_{\mathcal{T}})$ can estimate the complete domain classification error.

Subsequently, since the domain-invariant causality shared by both domains, and both terms has been reconstructed, a domain discriminator is introduced to recognize the decision boundary for source and target domains by given the reconstruction $\mathbf{R}_{t|\mathbf{a}_t}$. Shown in Corollary 1, a temporal loss function for domain classification error \mathcal{L}_{dom} is defined to compute the distance between source and target domains under treatment

policy \mathbf{a}_t ,

$$\begin{aligned} \mathcal{L}_{\text{dom}}(\mathcal{D}_{\mathcal{S}}, \mathcal{D}_{\mathcal{T}}, \mathcal{D}_{\mathcal{S}|\mathbf{Z}}, \mathcal{D}_{\mathcal{T}|\mathbf{Z}}; \mathcal{G}_{\mathcal{S}}, \mathcal{G}_{\mathcal{T}}) \\ = \left\| \frac{1}{|\mathcal{D}_{\mathcal{S}}|} \sum_{\mathbf{X}_t \in \mathcal{D}_{\mathcal{S}}} \mathbf{X}_t - \frac{1}{|\mathcal{D}_{\mathcal{T}}|} \sum_{\mathbf{X}_t \in \mathcal{D}_{\mathcal{T}}} \mathbf{X}_t \right\|_2^2 \\ + \left\| \frac{1}{|\mathcal{D}_{\mathcal{S}}|} \sum_{\mathbf{a}_t \in \mathbf{Z}} \sum_{\mathbf{X}_t \in \mathcal{D}_{\mathcal{S}|\mathbf{Z}}} \mathbf{R}_{t|\mathbf{a}_t} - \frac{1}{|\mathcal{D}_{\mathcal{T}}|} \sum_{\mathbf{a}_t \in \mathbf{Z}} \sum_{\mathbf{X}_t \in \mathcal{D}_{\mathcal{T}|\mathbf{Z}}} \mathbf{R}_{t|\mathbf{a}_t} \right\|_2^2 \\ + \left\| \frac{1}{|\mathcal{D}_{\mathcal{S}}|} \sum_{\mathbf{X}_t \in \mathcal{D}_{\mathcal{S}}} \mathbf{X}_t - \frac{1}{|\mathcal{D}_{\mathcal{S}|\mathbf{Z}}|} \sum_{\mathbf{a}_t \in \mathbf{Z}} \sum_{\mathbf{X}_t \in \mathcal{D}_{\mathcal{S}|\mathbf{Z}}} \mathbf{R}_{t|\mathbf{a}_t} \right\|_2^2 \\ + \left\| \frac{1}{|\mathcal{D}_{\mathcal{T}}|} \sum_{\mathbf{X}_t \in \mathcal{D}_{\mathcal{T}}} \mathbf{X}_t - \frac{1}{|\mathcal{D}_{\mathcal{T}|\mathbf{Z}}|} \sum_{\mathbf{a}_t \in \mathbf{Z}} \sum_{\mathbf{X}_t \in \mathcal{D}_{\mathcal{T}|\mathbf{Z}}} \mathbf{R}_{t|\mathbf{a}_t} \right\|_2^2 \end{aligned} \quad (16)$$

where $|\mathcal{X}^{\mathcal{S}}|$ and $|\mathcal{X}^{\mathcal{T}}|$ denote the cardinality associated with the source $\mathcal{D}_{\mathcal{S}}$ and target $\mathcal{D}_{\mathcal{T}}$.

Domain Adversarial Learning. Recalling the problem formulation, we have defined a joint treatment-outcome model Eq.(4) based on the shared causality and Markov model. The shared causality induces the domain-invariant features $\mathbf{R}_{t|\mathbf{a}_t}$ calculated by the answers of queries $\mathbf{A}|\mathbf{Z}$ and keys $\mathbf{K}|\text{CATE}$ across domains. While a domain discriminator tries to classify the domain between source and target data, the defined sequence generators in this section are trained to confuse the discriminator, aiming at the better generalization to a worst-case set of discriminator. By adopting the MSE loss for $l(\cdot)$, the minimax objective in Eq.(11) is now formally defined over generators $\mathcal{G}_{\mathcal{S}}, \mathcal{G}_{\mathcal{T}}$ with parameter $\Theta_{\mathcal{G}}$ and domain discriminator B with parameter Θ_B . Algorithm 1 summarized the training routine of CDA. The CDA alternately update the $\Theta_{\mathcal{G}}$ and Θ_B in opposite directions so that $\mathcal{G}_{\mathcal{S}}, \mathcal{G}_{\mathcal{T}}$ and B are trained adversarially. Here, $\hat{\mathbf{X}}, \hat{\mathbf{Y}}$ denote the predictive value of \mathbf{X}, \mathbf{Y} for sequence generators.

IV. EXPERIMENTAL VERIFICATION

In this section, we verify the effectiveness of the proposed CDA in adapting from source domain to target domain, and then estimate counterfactual outcome trajectories under treatment policy. The experiments proceeding in real-word oilfield dataset are composed of two parts, that is, time-series forecasting and the optimal policy exploiting for oil production, respectively.

A. Experimental Apparatus

Datasets in oil and gas industry. The target oil block, GD-NG52+3, is a typical sample of waterflooding oilfields in China. It is located in East China, which has well developed sand body and thick oil layer. The area of this block is about 9.1 km², with an average effective thickness of 7.9 m, holding the geological reserves of 13150 million tons. This block was developed by water flooding since 1986, which has a long history and adequate development data. Now it is at the stage of high water cut, which faces a critical issue about how to optimize the water inject/oil product scheme. The real-world oilfield datasets are sampled from the above oil block

Algorithm 1 Adversarial Training of CDA**Input:** datasets $\mathcal{D}_S, \mathcal{D}_T$, epoches E , setp sizes**Output:** Trained CDA forecaster parameterized by Θ_G and Θ_B

```

1: Initialization: parameters  $\Theta_G$  and  $\Theta_B$ 
2: for epoch = 1 to  $E$  do
3:   repeat
4:     sample  $(\mathbf{X}_S, \mathbf{Y}_S, \mathbf{Z}_S) \sim \mathcal{D}_S$  and  $(\mathbf{X}_T, \mathbf{Y}_T, \mathbf{Z}_T) \sim \mathcal{D}_T$ 
5:     generate  $\mathbf{R}_S, \hat{\mathbf{Y}}_S = \mathcal{G}_S(\mathbf{X}_S, \mathbf{Z}_S)$  and  $\mathbf{R}_T, \hat{\mathbf{Y}}_T = \mathcal{G}_T(\mathbf{X}_T, \mathbf{Z}_T)$ 
6:     compute  $\mathcal{L}_{seq}(\mathbf{Y}_S, \hat{\mathbf{Y}}_S), \mathcal{L}_{seq}(\mathbf{Y}_T, \hat{\mathbf{Y}}_T)$  for  $\mathcal{G}_S, \mathcal{G}_T, \mathcal{L}_{dom}(\mathbf{X}_S, \mathbf{X}_T, \mathbf{Z}_S, \mathbf{Z}_T)$  for  $B$   $\triangleright$  Using Eq.(16) and (12)
7:     compute  $\mathcal{L} = \mathcal{L}_{seq}(\mathbf{Y}_S, \hat{\mathbf{Y}}_S) + \mathcal{L}_{seq}(\mathbf{Y}_T, \hat{\mathbf{Y}}_T) + \lambda \mathcal{L}_{dom}(\mathbf{R}_S, \mathbf{R}_T, \mathbf{Z}_S, \mathbf{Z}_T)$   $\triangleright$  Using Eq.(11)
8:     gradient descent with  $\nabla_{\Theta_G} \mathcal{L}$  to update  $\mathcal{G}_S, \mathcal{G}_T$ 
9:     gradient descent with  $\nabla_{\Theta_B} \mathcal{L}$  to update  $B$ 
10:   until  $\mathcal{D}_T$  is exhausted
11: end for

```

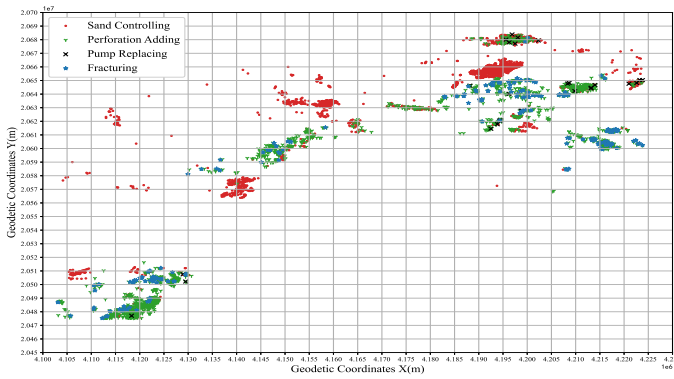


Fig. 4: The location of oil wells.

in Shandong Province, China. Notably, the oilfield dataset are synthetic exploitation and production monthly time-series of 1474 wells from 2001 to 2020, comprising a total of 353760 recods. The dataset contains 14 indicators, covering dynamical engineering variable \mathbf{X} , dynamical policy variable \mathbf{Z} , dynamical production variable \mathbf{Y} and static geological variable \mathbf{U} , shown in Table I. In oil and gas industry, the policy can be divided into the 4 typical classification, i.e., *Sand Controlling*, *Perforation Adding*, *Pump Replacing* and *Fracturing*, where the top 3 policies are the productive measure and the last policy is the protective policy. Thus, the dataset can be dividide to 4 partions according to the property of policy \mathbf{Z} . The characteristics of variables w.r.t. 4 partions are described in Table II

The ubiquity of temporal causality exists in oil and gas industry, but it is accompanied by the time lags and indirect causal effect due to the properties of oilfield exploitation. Specifically, oil production \mathbf{Y} has been demonstrated as lags in response when one of treatment policy \mathbf{Z} is applied in activity, and policy indirectly affects oil production \mathbf{Y} by directly influencing engineering factors \mathbf{X} .

Experimental settings The experiments consist of 3 independent phase for oil production \mathbf{Y} , including inside-well time-sereis forecasting, cross-well time-sereis predicting and optimal policy determining.

- The experiment, inside-well time-sereis forecasting, is to forecast the oil production in the coming months by utilizing the history time-series of whole oil wells.
- The experiment, cross-well time-sereis predicting, is to predict the oil production in the entire period by utilizing the history time-series of partial oil wells.
- The experiment, optimal policy determining, is to determine the optimal policy in improving oil production for a specifical well.

For inside-well time-sereis forecasting and cross-well time-sereis predicting, we compare CDA with the single-domain and cross-domain forecaster. The conventional single-domain forecasters trained only on source or target domain, including DecoderMLP, LSTM, GRU, Bi-LSTM, Bi-GRU, DeepAR and N-Beats. The cross-domain forecasters trained on both source and target domain, including Transformer, TFT, DANN, MMDA, SASA and our CDA. Specifically, for each experiment, the source domain \mathcal{D}_S is $[\mathbf{X}, \mathbf{Z}, \mathbf{U}]$ for the models TFT and ours, while the source domain of others \mathcal{D}_S is $[\mathbf{X}, \mathbf{Z}]$. In addition, R^2 score, Root Mean Square Error (RMSE) and Mean Absolute Error (MAE) are employed as evaluation metrics to assess the performance of models, which are as follows,

$$\begin{aligned}
 R^2 &= 1 - \text{SSE}/\text{SST} \\
 \text{RMSE} &= \left(\sum_{t=1}^n (\hat{y}_t - y_t) / n \right)^{1/2} \\
 \text{MAE} &= \frac{1}{n} \sum_{t=1}^n |\hat{y}_t - y_t|
 \end{aligned} \tag{17}$$

where $\text{SSE} = \sum_{t=1}^n (\hat{y}_t - y_t)^2$, $\text{SST} = \sum_{t=1}^n (\bar{y}_T - y_t)^2$; y_t, \hat{y}_t , and \bar{y}_T denote the actual value, predictive value, and mean value at timestep t .

B. Inside-well Time-series Forecasting

In this section, we mainly study the performance of temporal models in inside-wells time-series forecasting, which results are shown in Table III.

Experimental setup. In the phase of inside-well time-sereis forecasting, we characterize the last $\tau = 36, 24, 12, 6$ monthly time-series of each well as the target domain \mathcal{D}_T respectively, while the remained monthly time-series are formulized as source domain \mathcal{D}_S . The experiments consist of 4 independent

TABLE I: Categorization and variables of datasets

Category	Variables ¹	The Remarks of Z ²
Dynamical	X_1 , Days of produced (d), X_2 , Effective thickness (m), X_3 , Pump depth (m), X_4 , Pump diameter (m), X_5 , Pump efficiency (%), X_6 , Displacement (t) X_7 , Dynamic fluid interface (m) X_8 , Stroke (m), X_9 , Frequency of stroke (SPM), X_{10} , Casing pressure (MPa)	Sand Controlling , i.e., Protecting the relevant instruments of oil wells, and slightly improving the capacity of producing ; Perforation Adding , i.e., Enlarging the contact area of reservoir, and improving the skin factor; Pump Replacing , i.e., Changing the pressure difference in producing, and improving the capacity of supplying liquid; Fracturing , i.e., Improving the permeability, and enhancing the capacity of liquid flowing in the formation.
	Z_1 , Sand Controlling, Z_2 , Perforation Adding, Z_3 , Pump Replacing, Z_4 , Fracturing	
	Y , Monthly Oil Production (t)	
	U_1 , Formation temperature (°C), U_2 , Formation pressure (MPa)	
Static		

¹ The vectors $\mathbf{X} = \{X_1, X_2, \dots, X_{10}\}$, $\mathbf{Z} = \{Z_1, Z_2, Z_3, Z_4\}$, $\mathbf{U} = \{U_1, U_2\}$.

² (Can be classified into four types) The policies, including Perforation Adding, Pump Replacing and Fracturing, aim at improving the production capacity, while Sand Controlling is utilized to protect the instruments of oil wells.

TABLE II: The characteristics of oilfield datasets for 4 policies

Variables	Sand Controlling						Perforation Adding					
	min	max	mean	std	count	num	min	max	mean	std	count	num
X_1	0	31	20	12	234000	975	0	31	12	22	101760	424
X_2	0	2017.6	8.24	15.12	234000	975	0	455	17.59	12.1	101760	424
X_3	0	14149.3	950	281.1	234000	975	0	8960.6	452.2	1311	101760	424
X_4	0	997	62.05	27.4	234000	975	0	150	13.26	52.91	101760	424
X_5	0	212970	44.5	452.4	234000	975	0	48690	355.1	54.6	101760	424
X_6	0	17854.6	60.8	124.4	234000	975	0	4003.2	45.28	49.11	101760	424
X_7	1	8444	578.9	365.8	234000	975	1	8756	544.5	829.6	101760	424
X_8	0	99	3.46	6.27	234000	975	0	99	2.01	3.44	101760	424
X_9	0	306	10.5	21.94	234000	975	0	120	8.19	5.89	101760	424
X_{10}	0	240	1.14	3.64	234000	975	0	83	2.91	1.30	101760	424
Y	0	8221	151.7	238.7	234000	975	0	9135	206.1	141.3	101760	424
Variables	Pump Replacing						Fracturing					
	min	max	mean	std	count	num	min	max	mean	std	count	num
X_1	0	31	25	10	4560	19	0	31	22	12	13440	56
X_2	0	54.8	12.73	13.23	4560	19	0	133.2	15.74	18.7	13440	56
X_3	100	2938	1007	354.0	4560	19	0	2294	1694.3	285.2	13440	56
X_4	0	200	66.04	21.91	4560	19	0	83	45.01	7.11	13440	56
X_5	0	603.7	51.95	51.49	4560	19	0	4981	31.48	148.8	13440	56
X_6	0	275.4	88.97	55.40	4560	19	0	433.3	28.62	25.82	13440	56
X_7	1	4981	578.1	414	4560	19	2	9107	1226.8	546.3	13440	56
X_8	0.6	7.4	3.39	1.01	4560	19	0	7	3.66	1.29	13440	56
X_9	0	120	9.06	16.5	4560	19	0	73	6.34	10.04	13440	56
X_{10}	0	7.1	0.84	1	4560	19	0	60	1.59	3.22	13440	56
Y	0	4112	300.2	367.7	4560	19	0	3237	108.14	126.9	13440	56

mouldles, corresponding to the forecasting task involving *Sand Controlling*, *Perforation Adding*, *Pump Replacing* and *Fracturing*, respectively. For example, in the forecasting task of *Sand Controlling* with $\tau = 36$, the knowledge of last 36 monthly time-series involving *Sand Controlling* described in Table I is applied to transferred to the target domain \mathcal{D}_T , i.e. conducting the inside-well time-sereis forecasting of oil production.

The results in Table III demonstrate that the performance of CDA is better than or on par with the baselines under the different experimental apparatus. We note the following observations to provide a better understanding into inside-well time-series forecasting. First, for any forecasting tasks, the cross-domain forecasters (CDA, TFT, Transformer, DANN, MMDA and SASA) that jointly trained end-to-end using source and target domains outperform the single-domain forecasters (DecoderMLP, LSTM, GRU, Bi-LSTM, Bi-GRU, DeepAR and

N-Beats). The finding indicates that jointly training on source and target domain is helpful for inside-well time-series forecasting. Second, in the forecasting tasks of *Sand Controlling*, *Perforation Adding*, *Pump Replacing* and *Fracturing*, whatever with $\tau = 36, \tau = 24, \tau = 12$ or $\tau = 6$, TFT, Transformer and DANN, MMDA and SASA are outperformed by CDA. The finding illustrates that time-series forecaster under casuality and policy information is beneficial to achieve the better domain adaption in inside-well time-series forecasting.

C. Cross-well Time-sereis Predicting

In this section, we perform the extensive experiments to compare the proposed CDA with other models in cross-wells time-sereis predicting, which results are presented in Table IV. **Experimental setup.** In the phase of cross-well time-sereis predicting, the entire time-series of partial wells are denoted as

TABLE III: Performance comparison of multiple source domain knowledge in oil production forecasting of inside-well.

Sand Controlling												
Method	$\tau = 36$			$\tau = 24$			$\tau = 12$			$\tau = 6$		
	R^2	RMSE	MAE	R^2	RMSE	MAE	R^2	RMSE	MAE	R^2	RMSE	MAE
DecoderMLP	0.219	30.545	15.592	0.300	28.843	15.170	0.396	26.370	15.035	0.479	22.315	18.961
LSTM	0.240	29.665	23.089	0.827	14.671	6.820	0.696	19.848	11.365	0.751	15.240	12.365
GRU	0.547	22.897	13.650	0.644	20.419	10.783	0.724	18.558	13.953	0.762	15.078	13.126
Bi-LSTM	0.236	29.861	21.059	0.595	22.135	11.235	0.799	15.574	10.182	0.749	15.680	12.954
Bi-GRU	0.597	21.467	13.585	0.782	15.694	9.889	0.807	14.556	6.991	0.819	14.891	12.892
DeepAR	0.742	18.023	13.621	0.770	16.621	10.448	0.812	13.997	6.630	0.838	13.958	10.743
N-Beats	0.506	24.741	12.770	0.733	18.122	10.038	0.873	12.408	6.078	0.886	11.122	9.751
Transformer	0.826	14.565	9.265	0.839	14.195	8.782	0.817	13.835	6.271	0.895	10.742	8.378
DANN	0.631	20.578	12.041	0.795	15.178	9.471	0.837	14.058	7.648	0.892	10.342	7.971
SASA	0.672	20.280	11.612	0.821	14.606	9.190	0.866	12.523	6.146	0.911	8.464	6.716
TFT	0.869	12.554	7.554	0.913	9.293	8.583	0.923	8.763	5.675	0.935	6.884	4.559
MMDA	0.769	17.481	13.304	0.895	10.692	9.102	0.910	9.136	5.888	0.940	6.430	4.252
Ours	0.865	12.641	7.676	0.925	8.741	8.067	0.935	7.841	5.150	0.949	5.638	3.908
Perforation Adding												
Method	$\tau = 36$			$\tau = 24$			$\tau = 12$			$\tau = 6$		
	R^2	RMSE	MAE	R^2	RMSE	MAE	R^2	RMSE	MAE	R^2	RMSE	MAE
DecoderMLP	0.341	43.089	35.202	0.422	35.769	31.992	0.472	34.203	30.699	0.482	34.787	30.164
LSTM	0.449	35.260	30.290	0.512	31.004	26.979	0.492	33.642	29.677	0.495	33.208	28.907
GRU	0.487	33.168	28.587	0.537	30.050	26.685	0.526	30.942	27.754	0.580	28.181	22.819
Bi-LSTM	0.399	40.308	33.890	0.494	32.800	29.764	0.516	31.013	28.983	0.593	27.677	21.262
Bi-GRU	0.561	28.334	23.887	0.498	32.136	28.457	0.650	25.501	21.330	0.573	29.432	23.917
DeepAR	0.583	26.103	20.818	0.629	26.153	23.086	0.671	27.128	22.279	0.724	22.722	17.889
N-Beats	0.728	18.353	14.203	0.787	21.526	17.402	0.717	24.544	19.369	0.841	14.785	11.215
Transformer	0.754	17.035	13.469	0.805	19.028	15.297	0.835	16.818	12.704	0.886	9.510	5.902
DANN	0.652	22.058	17.515	0.670	25.482	21.198	0.863	12.715	9.426	0.874	10.435	6.356
SASA	0.821	14.719	10.658	0.843	14.814	11.677	0.829	17.255	13.522	0.891	8.175	4.781
TFT	0.850	13.714	10.722	0.867	11.657	8.397	0.884	9.832	6.299	0.906	7.263	4.159
MMDA	0.836	14.159	11.170	0.851	13.474	9.422	0.868	12.327	8.155	0.915	6.043	3.980
Ours	0.853	13.270	10.091	0.872	11.292	8.086	0.897	8.539	5.041	0.924	5.121	2.501
Pump Replacing												
Method	$\tau = 36$			$\tau = 24$			$\tau = 12$			$\tau = 6$		
	R^2	RMSE	MAE	R^2	RMSE	MAE	R^2	RMSE	MAE	R^2	RMSE	MAE
DecoderMLP	0.252	28.944	20.146	0.304	26.093	17.620	0.405	21.689	10.905	0.426	16.684	8.739
LSTM	0.281	27.256	19.884	0.323	25.731	16.557	0.458	19.321	9.611	0.481	15.648	7.510
GRU	0.435	22.638	15.154	0.481	22.203	14.883	0.454	19.745	9.891	0.502	14.423	7.132
Bi-LSTM	0.430	22.852	15.443	0.515	21.009	13.275	0.550	16.118	9.214	0.564	12.220	6.528
Bi-GRU	0.451	22.128	15.055	0.529	20.988	12.987	0.563	15.963	8.871	0.598	11.780	6.186
DeepAR	0.517	20.882	14.819	0.578	19.869	12.866	0.595	15.307	8.214	0.636	9.921	5.631
N-Beats	0.590	19.402	13.333	0.682	16.047	10.881	0.720	10.980	5.975	0.779	7.410	4.371
Transformer	0.633	18.334	11.682	0.698	15.076	10.303	0.732	10.497	5.062	0.807	6.023	3.374
DANN	0.638	17.191	10.692	0.601	18.798	11.667	0.652	12.922	7.182	0.717	7.925	4.961
SASA	0.610	18.933	12.030	0.810	9.982	5.038	0.765	10.063	5.180	0.814	5.618	3.002
TFT	0.673	15.350	7.757	0.788	12.093	6.135	0.802	8.621	3.756	0.830	5.333	2.739
MMDA	0.682	15.814	7.933	0.798	11.281	6.983	0.825	7.201	3.728	0.841	4.626	2.126
Ours	0.724	13.159	5.111	0.813	9.514	4.461	0.836	6.412	2.156	0.859	4.098	1.822
Fracturing												
Method	$\tau = 36$			$\tau = 24$			$\tau = 12$			$\tau = 6$		
	R^2	RMSE	MAE	R^2	RMSE	MAE	R^2	RMSE	MAE	R^2	RMSE	MAE
DecoderMLP	0.316	22.837	15.188	0.389	25.080	15.208	0.453	16.752	8.873	0.497	14.590	9.806
LSTM	0.384	21.674	14.973	0.423	22.540	14.412	0.503	15.428	8.180	0.568	12.101	8.704
GRU	0.493	17.593	10.629	0.514	19.187	13.605	0.573	14.215	7.845	0.589	11.287	8.050
Bi-LSTM	0.487	18.037	11.509	0.561	17.979	11.273	0.586	13.357	7.236	0.667	9.717	6.287
Bi-GRU	0.533	16.997	9.695	0.592	16.649	10.867	0.677	10.450	5.762	0.696	9.042	6.127
DeepAR	0.554	16.329	9.314	0.569	15.087	10.050	0.651	11.032	6.388	0.725	7.297	5.157
N-Beats	0.683	15.774	8.991	0.736	12.537	8.224	0.801	7.678	4.484	0.827	5.131	3.331
Transformer	0.749	14.031	7.041	0.808	10.551	6.954	0.816	6.687	3.867	0.837	4.874	2.981
DANN	0.728	14.835	7.238	0.759	11.552	7.760	0.771	9.180	5.349	0.808	6.439	4.606
SASA	0.769	13.869	6.784	0.816	9.698	6.679	0.845	5.093	2.687	0.859	4.682	2.848
TFT	0.812	11.811	5.973	0.869	7.853	4.704	0.887	5.059	2.476	0.872	4.135	2.095
MMDA	0.824	11.241	5.477	0.859	7.680	4.679	0.866	5.340	2.340	0.887	3.447	1.840
Ours	0.842	11.003	4.307	0.870	7.004	4.420	0.897	4.362	2.059	0.912	3.073	1.339

the source domain \mathcal{D}_S , while the remained wells' entire time-series are remarked as target domain \mathcal{D}_T . The experiments also consist of 4 independent mouldles, corresponding to the forecasting task involving *Sand Controlling*, *Perforation Adding*, *Pump Replacing* and *Fracturing*, respectively. For

the instance, in the forecasting task of *Sand Controlling*, the target domain \mathcal{D}_T is the dataset described in Table I involving *Sand Controlling*. And for its source domain \mathcal{D}_S , $\not\subseteq \mathbf{Z}$ represents that the source domain \mathcal{D}_S does not contain any knowledge of *Sand Controlling*, while $\subseteq \mathbf{Z}$ represents that

the certain knowledge of *Sand Controlling* in source domain \mathcal{D}_S is transferred to the target domain \mathcal{D}_T , i.e., conducting the cross-well time-series predicting of oil production.

The results in Table IV also demonstrate the performance of CDA is better than or on par with the baselines under the corresponding experimental apparatus. There are also some observations that can provide a better understanding into cross-well time-series predicting. First, the cross-domain forecaster TFT, Transformer, MMDA, SASA and CDA outperform the single-domain forecaster DecoderMLP, LSTM, GRU, Bi-LSTM, Bi-GRU, DeepAR and N-Beats in two domain adaptation tasks. The finding indicates that jointly training on source and target domains is also helpful in cross-well time-series predicting. Second, the cross-domain forecaster, TFT, Transformer, DANN, and MMDA, are outperformed by CDA, indicating that domain adaptation combined with causal inference is beneficial to achieve the better performance in cross-well time-series predicting. Third, the predicting performance of our CDA is better than or competitive to other models in industrial cross-well time-series predicting.

Significantly, the observations of Table III and IV demonstrate the effectiveness of domain adaptation combined with causal inference, since it can capture the knowledge of policy-invariant representation under causality. Moreover, the results in Fig.5 illustrate that our method has achieved a better accuracy, especially in treatment region. In oil and gas industry, the main purpose of applying policy is to improve oil production. Thus, based on intermediate result of counterfactual inference, Position-wise CATE in Definition 1, our proposed CDA can provide a guidance in determining a optimal policy for improving oil production. The interpretable results are displayed in following section.

D. Optimal Policy Determining

In this section, we characterize our CDA on realizations of a synthetic decision-making process, mainly quantifying the causal effect of treatment policy \mathbf{Z} impacting on oil production \mathbf{Y} , and determining the optimal policy. To this end, we first estimate the outcome improvement that could have been achieved if treatment policies had been different to the observed ones in the treatment region, as dictated by the optimal treatment policy and intervention. Then, we decode (hypothetical) future treatment policy to determine its latent state and use this to predict counterfactual outcome and proceed the optimal treatment policy for improving oil production.

As shown in the Top of Fig.6, it summarizes the results for the CATE where an individual waterflooding well is intervened by different policy in treatment region and for the guidance where CATE is utilized to decide whether the policy is reasonable or not. Compared with the true oil production under the actual policy *Perforation Adding* in Fig.6(a), there are some observations in Fig.6(b) that can provide a better understanding into optimal policy in treatment region. First, since the the CATEs (< 0) of *Pump Replacing* and *Fracturing* in first treatment region (orange rectangles) are both less than bias CATE ($= 0$, the CATE of actual policy *Perforation*

Adding) we can guess that the policies *Pump Replacing* and *Fracturing* are ineffective treatment. for improving oil production in first treatment region. Second, since the CATE (< 0) of *Pump Replacing* is less than bias CATE ($= 0$, the CATE of actual policy *Perforation Adding*) and the CATE of *Fracturing* is almost more than bias CATE ($= 0$, the CATE of actual policy *Perforation Adding*) in second treatment region, these results illustrate that the policies *Pump Replacing* is ineffective treatment and the policies *Fracturing* is more valuable treatment than policy *Perforation Adding* for improving oil production in second treatment region.

In the left of Fig.7, we provide the predicted production trajectories for the treatment policies *Sucker Rod Pump* and *Perforation Adding*. And in the right of Fig.??, we provide the cumulative increment of predicted production (the response of the left Fig.7) under the treatment policies *Sucker Rod Pump* and *Perforation Adding*. Then, there are some guidance for improving of oil production. First, for Well 1, *Sucker Rod Pump* has more significant and positive causal effects in achieving the increment of oil production compared with *Perforation Adding*, which is corresponding to the top of Fig.??, while the reverse hold false for Well 2. Second, the predicted production and its CATE by CDA is an effective metric in guiding producing activity.

V. CONCLUSION

In this paper, we aim to combine domain adaptation with causal inference to industrial time-series forecasting to solve the data scarcity and decision-confusing. We identify the shared causality over time in both domains, which related theoretical analysis reveals the latent cause of domain shift from the perspective of casual inference, and accordingly propose a Causal Domain Adaptation (CDA) forecaster based on answer-based attention mechanism, which is more line with industrial production process. Different from the existing paradigm of time-series forecaster, CDA not only can perform industrial time-series forecasting across domains even with different treatments

but also can provide a guidance in industrial production process along with treatments. Through empirical experiments in real-word and synthetic oilfield datasets, we have demonstrated that CDA outperforms various single-domain and domain adaptation methods. We further show that the effectiveness of our designs in answering casual queries about the interventional and counterfactual distribution of outcome in guiding industrial production process.

REFERENCES

- [1] Q. Wang, S. Bu, Z. He, and Z. Y. Dong, "Toward the prediction level of situation awareness for electric power systems using cnn-lstm network," *IEEE Transactions on Industrial Informatics*, vol. 17, no. 10, pp. 6951–6961, 2020.
- [2] C.-L. Liu, W.-H. Hsiao, and Y.-C. Tu, "Time series classification with multivariate convolutional neural network," *IEEE Transactions on industrial electronics*, vol. 66, no. 6, pp. 4788–4797, 2018.
- [3] M. Canizo, I. Triguero, A. Conde, and E. Onieva, "Multi-head cnn-rnn for multi-time series anomaly detection: An industrial case study," *Neurocomputing*, vol. 363, pp. 246–260, 2019.
- [4] O. I. Abiodun, A. Jantan, A. E. Omolara, K. V. Dada, N. A. Mohamed, and H. Arshad, "State-of-the-art in artificial neural network applications: A survey," *Heliyon*, vol. 4, no. 11, 2018.

TABLE IV: Performance comparison of multiple source domain knowledge in oil production forecasting of cross-well.

Measure	Sand Controlling						Perforation Adding					
Method	$\not\subseteq Z$			$\subseteq Z$			$\not\subseteq Z$			$\subseteq Z$		
	R^2	RMSE	MAE	R^2	RMSE	MAE	R^2	RMSE	MAE	R^2	RMSE	MAE
DecoderMLP	0.372	41.911	22.941	0.829	16.844	12.043	0.528	32.660	26.217	0.824	23.064	15.340
LSTM	0.535	33.500	13.888	0.835	16.483	11.971	0.539	30.957	25.731	0.906	16.580	14.518
GRU	0.571	31.367	16.357	0.837	15.267	11.187	0.381	43.327	35.742	0.908	16.638	14.333
Bi-LSTM	0.448	38.270	20.489	0.844	13.628	10.217	0.580	28.884	22.240	0.850	20.241	11.275
Bi-GRU	0.556	32.259	15.485	0.862	12.408	10.063	0.563	21.780	17.045	0.859	20.159	11.111
DeepAR	0.849	20.480	14.319	0.881	11.792	8.775	0.584	26.484	20.351	0.912	15.425	10.002
N-Beats	0.775	29.388	17.849	0.923	8.692	7.820	0.774	18.837	14.240	0.945	12.272	8.980
Transformer	0.856	19.716	13.689	0.851	9.938	7.830	0.860	16.270	21.992	0.953	12.256	6.677
DANN	0.672	24.988	12.881	0.890	10.214	7.772	0.681	20.729	17.144	0.948	12.071	8.523
SASA	0.827	22.947	9.738	0.919	8.858	6.080	0.740	18.860	14.455	0.941	13.645	7.861
TFT	0.834	21.456	8.972	0.924	8.866	6.052	0.642	24.622	20.690	0.950	12.596	7.818
MMDA	0.861	17.962	7.167	0.930	8.802	5.584	0.832	16.437	12.825	0.952	12.055	7.529
Ours	0.875	14.771	6.026	0.935	7.694	5.196	0.886	16.110	12.366	0.953	11.719	6.679

Measure	Pump Replacing						Fracturing					
Method	$\not\subseteq Z$			$\subseteq Z$			$\not\subseteq Z$			$\subseteq Z$		
	R^2	RMSE	MAE	R^2	RMSE	MAE	R^2	RMSE	MAE	R^2	RMSE	MAE
DecoderMLP	0.353	38.545	30.199	0.919	13.381	6.753	0.413	23.760	17.329	0.809	11.405	5.668
LSTM	0.471	27.605	20.148	0.947	12.017	6.114	0.501	18.313	14.682	0.937	9.893	4.674
GRU	0.484	25.301	18.909	0.941	12.176	5.612	0.518	17.844	11.957	0.955	7.178	3.462
Bi-LSTM	0.408	33.401	24.153	0.932	11.325	5.366	0.465	20.884	14.257	0.959	7.803	3.213
Bi-GRU	0.484	25.587	17.779	0.936	11.357	4.818	0.532	17.287	12.891	0.945	9.441	4.660
DeepAR	0.502	23.173	15.129	0.966	10.684	4.804	0.621	16.005	11.707	0.947	9.265	4.024
N-Beats	0.740	18.839	12.650	0.962	9.205	3.914	0.754	14.062	9.211	0.969	7.697	3.386
Transformer	0.781	18.470	11.068	0.962	8.727	3.987	0.765	13.821	8.659	0.966	7.893	3.414
DANN	0.639	20.430	13.897	0.968	9.190	3.733	0.681	15.206	10.455	0.974	6.537	2.029
SASA	0.751	18.605	11.672	0.969	8.247	3.505	0.787	13.664	8.730	0.976	6.531	1.841
TFT	0.774	18.026	11.700	0.971	7.079	3.113	0.819	11.813	6.879	0.970	6.048	1.736
MMDA	0.806	16.366	9.162	0.970	7.754	3.144	0.826	11.655	6.545	0.976	5.593	1.709
Ours	0.828	15.318	8.467	0.971	7.195	3.936	0.836	10.944	5.917	0.981	5.506	1.477

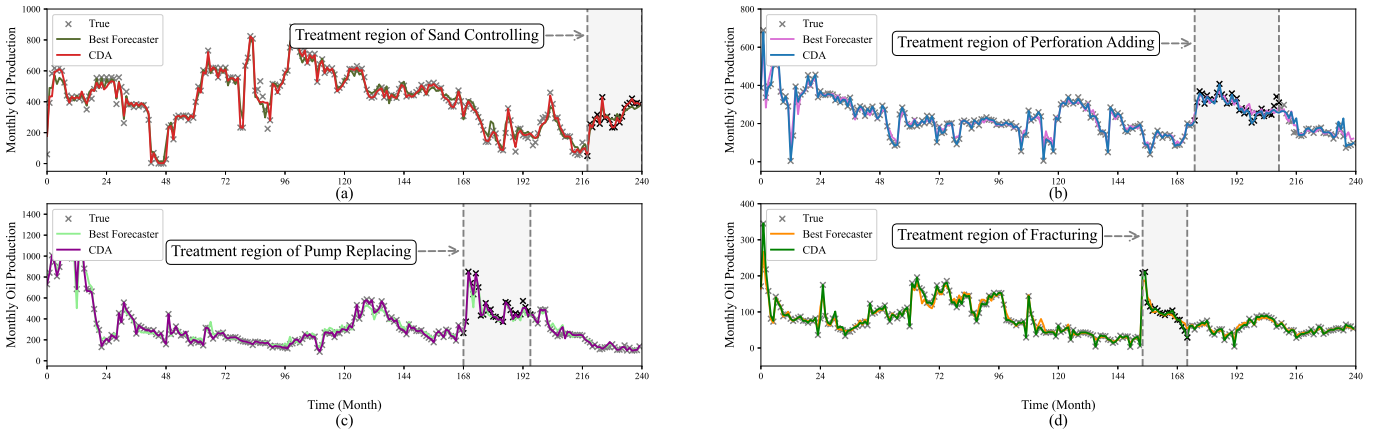


Fig. 5: Performance comparison of CFDA, best single-domain forecaster and cross-domain forecaster in estimating treatment-outcome

- [5] Z. Li, R. Cai, H. W. Ng, M. Winslett, T. Z. Fu, B. Xu, X. Yang, and Z. Zhang, "Causal mechanism transfer network for time series domain adaptation in mechanical systems," *ACM Transactions on Intelligent Systems and Technology (TIST)*, vol. 12, no. 2, pp. 1–21, 2021.
- [6] N. Al-Bulushi, P. King, M. J. Blunt, and M. Kraaijveld, "Artificial neural networks workflow and its application in the petroleum industry," *Neural Computing and Applications*, vol. 21, pp. 409–421, 2012.
- [7] D. Fooshee, A. Mood, E. Gutman, M. Tavakoli, G. Urban, F. Liu, N. Huynh, D. Van Vranken, and P. Baldi, "Deep learning for chemical reaction prediction," *Molecular Systems Design & Engineering*, vol. 3, no. 3, pp. 442–452, 2018.
- [8] M. Wainberg, D. Merico, A. Delong, and B. J. Frey, "Deep learning in biomedicine," *Nature biotechnology*, vol. 36, no. 9, pp. 829–838, 2018.
- [9] A. Vaswani, N. Shazeer, N. Parmar, J. Uszkoreit, L. Jones, A. N. Gomez, E. Kaiser, and I. Polosukhin, "Attention is all you need," *Advances in neural information processing systems*, vol. 30, 2017.
- [10] X. Zhou, N. Zhai, S. Li, and H. Shi, "Time series prediction method of industrial process with limited data based on transfer learning," *IEEE Transactions on Industrial Informatics*, 2022.
- [11] M. Bertolini, D. Mezzogori, M. Neroni, and F. Zammori, "Machine learning for industrial applications: A comprehensive literature review," *Expert Systems with Applications*, vol. 175, p. 114820, 2021.
- [12] Y. Bengio, "Deep learning of representations for unsupervised and transfer learning," in *Proceedings of ICML workshop on unsupervised and transfer learning*. JMLR Workshop and Conference Proceedings, 2012, pp. 17–36.
- [13] B. Lim, S. Ö. Arık, N. Loeff, and T. Pfister, "Temporal fusion transformers for interpretable multi-horizon time series forecasting," *International Journal of Forecasting*, vol. 37, no. 4, pp. 1748–1764, 2021.
- [14] R. Wang, D. Maddix, C. Faloutsos, Y. Wang, and R. Yu, "Bridging physics-based and data-driven modeling for learning dynamical systems," in *Learning for Dynamics and Control*. PMLR, 2021, pp. 385–

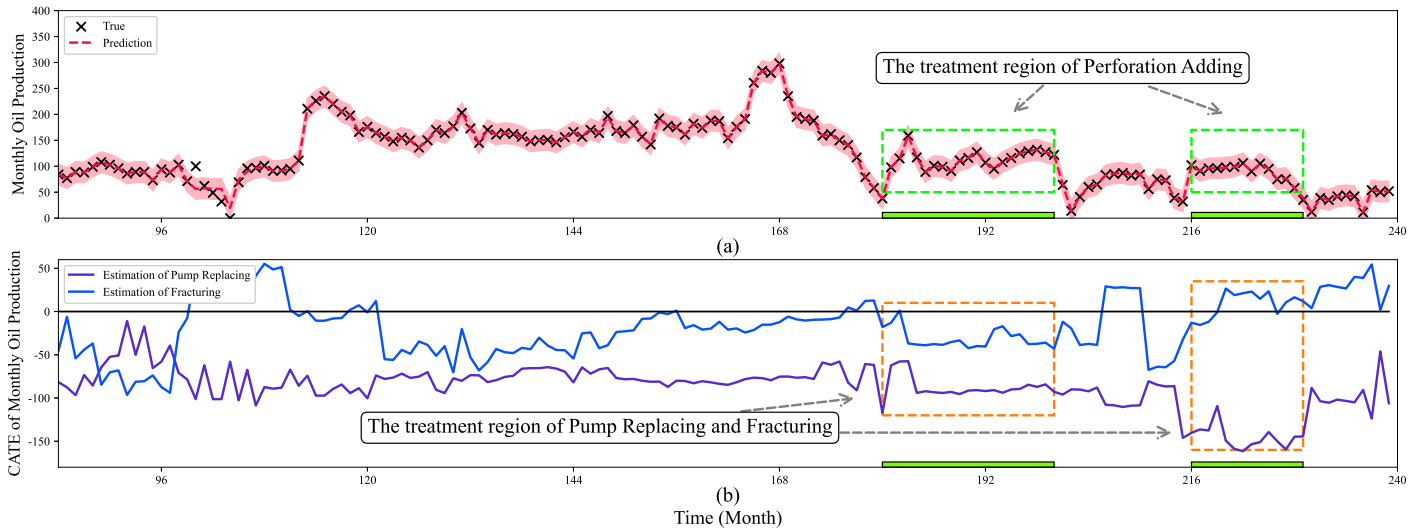


Fig. 6: The treatment region of policy and CATE of oil production. **Fig.6(a):** The treatment region under the policy *Perforation Adding*, where the points in green rectangles denote the response of oil production under the policy *Perforation Adding*. **Fig.6(b):** The CATE of oil production under the policies *Pump Replacing* and *Fracturing*, where the points in orange rectangles denote the CATE of oil production under the policies *Pump Replacing* and *Fracturing* and the black line denotes the CATE of actual policy *Perforation Adding*.

398.

- [15] E. Tzeng, J. Hoffman, K. Saenko, and T. Darrell, "Adversarial discriminative domain adaptation," in *Proceedings of the IEEE conference on computer vision and pattern recognition*, 2017, pp. 7167–7176.
- [16] S. Niu, Y. Liu, J. Wang, and H. Song, "A decade survey of transfer learning (2010–2020)," *IEEE Transactions on Artificial Intelligence*, vol. 1, no. 2, pp. 151–166, 2020.
- [17] Y. Ganin, E. Ustinova, H. Ajakan, P. Germain, H. Larochelle, F. Laviolette, M. March, and V. Lempitsky, "Domain-adversarial training of neural networks," *Journal of machine learning research*, vol. 17, no. 59, pp. 1–35, 2016.
- [18] M. M. Rahman, C. Fookes, M. Baktashmotlagh, and S. Sridharan, "On minimum discrepancy estimation for deep domain adaptation," *Domain Adaptation for Visual Understanding*, pp. 81–94, 2020.
- [19] Y. Zhang, T. Liu, M. Long, and M. Jordan, "Bridging theory and algorithm for domain adaptation," in *International conference on machine learning*. PMLR, 2019, pp. 7404–7413.
- [20] M. Ragab, E. Eldele, W. L. Tan, C.-S. Foo, Z. Chen, M. Wu, C.-K. Kwoh, and X. Li, "Adatime: A benchmarking suite for domain adaptation on time series data," *ACM Transactions on Knowledge Discovery from Data*, vol. 17, no. 8, pp. 1–18, 2023.
- [21] Y. Wang, Y. Xu, J. Yang, Z. Chen, M. Wu, X. Li, and L. Xie, "Sensor alignment for multivariate time-series unsupervised domain adaptation," in *Proceedings of the AAAI Conference on Artificial Intelligence*, vol. 37, no. 8, 2023, pp. 10 253–10 261.
- [22] G. Wilson and D. J. Cook, "A survey of unsupervised deep domain adaptation," *ACM Transactions on Intelligent Systems and Technology (TIST)*, vol. 11, no. 5, pp. 1–46, 2020.
- [23] S. Kan, B. Chen, J. Meng, and G. Chen, "An extended overview of natural gas use embodied in world economy and supply chains: Policy implications from a time series analysis," *Energy Policy*, vol. 137, p. 111068, 2020.
- [24] F. Bilgili, E. Koçak, Ü. Bulut, and M. N. Sualp, "How did the us economy react to shale gas production revolution? an advanced time series approach," *Energy*, vol. 116, pp. 963–977, 2016.
- [25] X. Zhang, C. Song, J. Zhao, Z. Xu, and X. Deng, "Spatial-temporal causality modeling for industrial processes with a knowledge-data guided reinforcement learning," *IEEE Transactions on Industrial Informatics*, 2023.
- [26] B. Cai, L. Huang, and M. Xie, "Bayesian networks in fault diagnosis," *IEEE Transactions on industrial informatics*, vol. 13, no. 5, pp. 2227–2240, 2017.
- [27] H. Wang, R. Liu, S. X. Ding, Q. Hu, Z. Li, and H. Zhou, "Causal-trivial attention graph neural network for fault diagnosis of complex industrial processes," *IEEE Transactions on Industrial Informatics*, 2023.
- [28] J. Li, B. Yang, H. Li, Y. Wang, C. Qi, and Y. Liu, "Dtdr-alstm: Extracting dynamic time-delays to reconstruct multivariate data for improving attention-based lstm industrial time series prediction models," *Knowledge-Based Systems*, vol. 211, p. 106508, 2021.
- [29] Z. Li, R. Cai, T. Z. Fu, Z. Hao, and K. Zhang, "Transferable time-series forecasting under causal conditional shift," *IEEE Transactions on Pattern Analysis and Machine Intelligence*, 2023.
- [30] J. D. Correa, S. Lee, and E. Bareinboim, "Counterfactual transportability: a formal approach," in *International Conference on Machine Learning*. PMLR, 2022, pp. 4370–4390.
- [31] G. W. Imbens and D. B. Rubin, *Causal inference in statistics, social, and biomedical sciences*. Cambridge University Press, 2015.
- [32] S. Magliacane, T. Van Ommen, T. Claassen, S. Bongers, P. Versteeg, and J. M. Mooij, "Domain adaptation by using causal inference to predict invariant conditional distributions," *Advances in neural information processing systems*, vol. 31, 2018.
- [33] X. Jin, Y. Park, D. Maddix, H. Wang, and Y. Wang, "Domain adaptation for time series forecasting via attention sharing," in *International Conference on Machine Learning*. PMLR, 2022, pp. 10 280–10 297.
- [34] T. Teshima, I. Sato, and M. Sugiyama, "Few-shot domain adaptation by causal mechanism transfer," in *International Conference on Machine Learning*. PMLR, 2020, pp. 9458–9469.
- [35] F. Johansson, U. Shalit, and D. Sontag, "Learning representations for counterfactual inference," in *International conference on machine learning*. PMLR, 2016, pp. 3020–3029.
- [36] S. J. Pan, I. W. Tsang, J. T. Kwok, and Q. Yang, "Domain adaptation via transfer component analysis," *IEEE transactions on neural networks*, vol. 22, no. 2, pp. 199–210, 2010.
- [37] Ç. Hızı, S. John, A. T. Juuti, T. T. Saarinen, K. H. Pietiläinen, and P. Marttinen, "Causal modeling of policy interventions from treatment-outcome sequences," in *International Conference on Machine Learning*. PMLR, 2023, pp. 13 050–13 084.
- [38] T. Hatt and S. Feuerriegel, "Sequential deconfounding for causal inference with unobserved confounders," *arXiv preprint arXiv:2104.09323*, 2021.
- [39] A. Gretton, K. M. Borgwardt, M. J. Rasch, B. Schölkopf, and A. Smola, "A kernel two-sample test," *The Journal of Machine Learning Research*, vol. 13, no. 1, pp. 723–773, 2012.
- [40] A. Kumagai and T. Iwata, "Unsupervised domain adaptation by matching distributions based on the maximum mean discrepancy via unilateral transformations," in *Proceedings of the AAAI Conference on Artificial Intelligence*, vol. 33, no. 01, 2019, pp. 4106–4113.

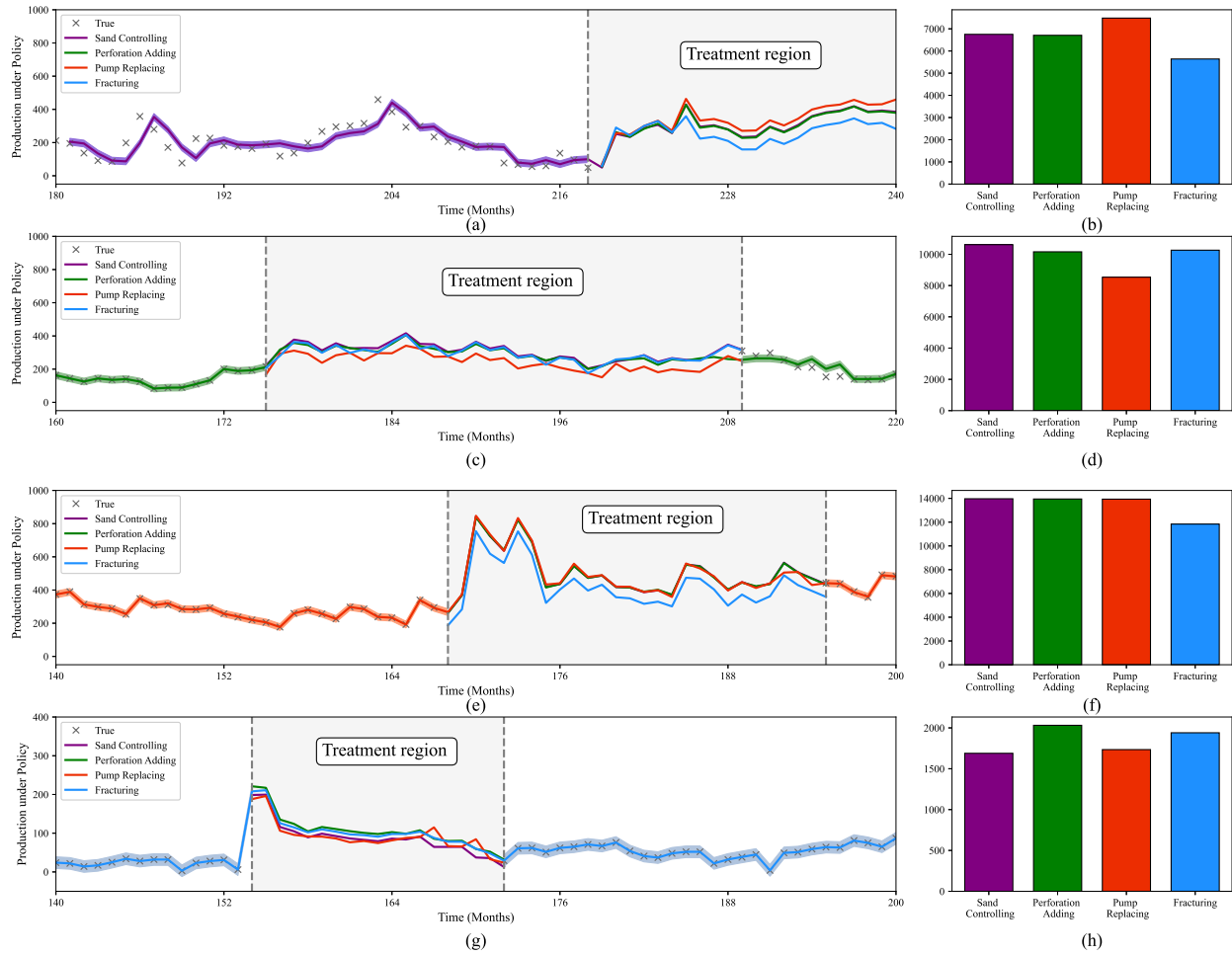


Fig. 7: Inside-Well Inference and Guidance for oil production under different treatment policy. **Left in Top:** The predicted oil production of Well 1 under treatment policy, where purple line denote the actual oil production without any treatment policy. **Left in Bottom:** The predicted oil production of Well 2 under treatment policy, where purple line denote the actual oil production without any treatment policy. **Right in Top:** The cumulative increment of oil production under treatment policy for Well 1. **Right in Bottom:** The cumulative increment of oil production under treatment policy for Well 2.

APPENDIX

In this section, we give the proof of the Theorem 1.

Theorem 1. Let $\mu[P]$ be a distribution of P in RKHS \mathcal{H}_k , then via the reproducing property of RKHS \mathcal{H}_k , we have $\langle \phi, \mu[P_{\mathcal{T}, \mathcal{S}}] \rangle = \mathbb{E}_{\mathbf{X} \sim \mathcal{T}, \mathcal{S}}[\phi(\mathbf{X})]$ for MMD, $\langle \phi, \mu[P_{\mathcal{T}, \mathcal{S}|\mathbf{Z}}] \rangle = \mathbb{E}_{\mathbf{X} \sim \mathcal{T}, \mathcal{S}}[\phi(\mathbf{X}|\mathbf{Z})]$ for CMMD. Thus, the empirical estimate of squared CMMD shown in Definition 3 can be further simplified as

$$\begin{aligned} & d_{\text{CMMD}}^2(\mathcal{S}|\mathbf{Z}, \mathcal{T}|\mathbf{Z}) \\ & \leq \frac{1}{4} [d_{\text{CMMD}}^2(\mathcal{S}|\mathbf{Z}, \mathcal{T}|\mathbf{Z}) + d_{\text{CMMD}}^2(\mathcal{S}, \mathcal{S}|\mathbf{Z}) + d_{\text{CMMD}}^2(\mathcal{T}, \mathcal{T}|\mathbf{Z}) + d_{\text{MMD}}^2(\mathcal{S}, \mathcal{T}) + 2d_{\text{CMMD}}(\mathcal{S}|\mathbf{Z}, \mathcal{T}|\mathbf{Z})d_{\text{MMD}}(\mathcal{S}, \mathcal{T})] \end{aligned}$$

where d_{MMD} is the standard Maximum Mean Distance (MMD), $d_{\text{CMMD}}(\mathcal{S}, \mathcal{S}|\mathbf{Z})$ is applied to measure the closeness of source domain between the raw distributions $P_{\mathcal{S}}$ and condition distribution $P_{\mathcal{S}|\mathbf{Z}}$, and $d_{\text{CMMD}}(\mathcal{T}, \mathcal{T}|\mathbf{Z})$ is applied to measure the closeness of target domain between the raw distributions $P_{\mathcal{T}}$ and condition distribution $P_{\mathcal{T}|\mathbf{Z}}$.

Proof. Given the distributions of source $P_{\mathcal{S}}$ and target domain $P_{\mathcal{T}}$ [39], [40], its MMD can be defined as

$$d_{\text{MMD}}(\mathcal{S}, \mathcal{T}) = \|\mu(P_{\mathcal{S}}) - \mu(P_{\mathcal{T}})\|_{\mathcal{H}_k} \quad (18)$$

In addition, since $\langle \phi, \mu[P_{\mathcal{T}, \mathcal{S}}] \rangle = \mathbb{E}_{\mathbf{X} \sim \mathcal{T}, \mathcal{S}}[\phi(\mathbf{X})]$ in MMD and $\langle \phi, \mu[P_{\mathcal{T}, \mathcal{S}|\mathbf{Z}}] \rangle = \mathbb{E}_{\mathbf{X} \sim \mathcal{T}, \mathcal{S}}[\phi(\mathbf{X}|\mathbf{Z})]$ in CMMD, we have the following equations for CMMD

$$\begin{aligned} d_{\text{CMMD}}(\mathcal{S}|\mathbf{Z}, \mathcal{T}|\mathbf{Z}) &= \|\mu(P_{\mathcal{S}|\mathbf{Z}}) - \mu(P_{\mathcal{T}|\mathbf{Z}})\|_{\mathcal{H}_k} \\ d_{\text{CMMD}}(\mathcal{S}, \mathcal{S}|\mathbf{Z}) &= \|\mu(P_{\mathcal{S}}) - \mu(P_{\mathcal{S}|\mathbf{Z}})\|_{\mathcal{H}_k} \\ d_{\text{CMMD}}(\mathcal{T}, \mathcal{T}|\mathbf{Z}) &= \|\mu(P_{\mathcal{T}}) - \mu(P_{\mathcal{T}|\mathbf{Z}})\|_{\mathcal{H}_k} \end{aligned} \quad (19)$$

Thus, we can obtain

$$\begin{aligned} & d_{\text{CMMD}}(\mathcal{S}, \mathcal{T}|\mathbf{Z}) \\ &= \|\mu(P_{\mathcal{S}|\mathbf{Z}}) - \mu(P_{\mathcal{T}|\mathbf{Z}})\|_{\mathcal{H}_k} \\ &= \|\mu(P_{\mathcal{S}|\mathbf{Z}}) - \mu(P_{\mathcal{T}|\mathbf{Z}}) - \mu(P_{\mathcal{S}}) + \mu(P_{\mathcal{T}}) + \mu(P_{\mathcal{S}}) - \mu(P_{\mathcal{T}})\|_{\mathcal{H}_k} \\ &= \|\mu(P_{\mathcal{S}|\mathbf{Z}}) - \mu(P_{\mathcal{S}}) + [\mu(P_{\mathcal{S}}) - \mu(P_{\mathcal{T}|\mathbf{Z}})] + [\mu(P_{\mathcal{S}}) - \mu(P_{\mathcal{T}})]\|_{\mathcal{H}_k} \\ &\leq \|\mu(P_{\mathcal{S}|\mathbf{Z}}) - \mu(P_{\mathcal{S}})\|_{\mathcal{H}_k} + \|\mu(P_{\mathcal{T}|\mathbf{Z}}) - \mu(P_{\mathcal{T}})\|_{\mathcal{H}_k} + \|\mu(P_{\mathcal{S}}) - \mu(P_{\mathcal{T}})\|_{\mathcal{H}_k} \\ &= d_{\text{CMMD}}(\mathcal{S}, \mathcal{S}|\mathbf{Z}) + d_{\text{CMMD}}(\mathcal{T}, \mathcal{T}|\mathbf{Z}) + d_{\text{MMD}}(\mathcal{S}, \mathcal{T}) \end{aligned} \quad (20)$$

Let $d_{\text{CMMD}}(\mathcal{S}, \mathcal{T}|\mathbf{Z}) := \sup_{\|\phi\|_{\mathcal{H}_k} \leq 1} (d_{\text{CMMD}}(\mathcal{S}, \mathcal{S}|\mathbf{Z}) + d_{\text{CMMD}}(\mathcal{T}, \mathcal{T}|\mathbf{Z}) + d_{\text{MMD}}(\mathcal{S}, \mathcal{T}))$, the nearly minimal estimation of CMMD can be represented as

$$\begin{aligned} & d_{\text{CMMD}}^2(\mathcal{S}|\mathbf{Z}, \mathcal{T}|\mathbf{Z}) \\ &= \frac{1}{4} [d_{\text{CMMD}}(\mathcal{S}|\mathbf{Z}, \mathcal{T}|\mathbf{Z}) + d_{\text{CMMD}}(\mathcal{S}, \mathcal{S}|\mathbf{Z}) + d_{\text{CMMD}}(\mathcal{T}, \mathcal{T}|\mathbf{Z}) + d_{\text{MMD}}(\mathcal{S}, \mathcal{T})]^2 \\ &= \frac{1}{4} [d_{\text{CMMD}}^2(\mathcal{S}|\mathbf{Z}, \mathcal{T}|\mathbf{Z}) + d_{\text{CMMD}}^2(\mathcal{S}, \mathcal{S}|\mathbf{Z}) + d_{\text{CMMD}}^2(\mathcal{T}, \mathcal{T}|\mathbf{Z}) + d_{\text{MMD}}^2(\mathcal{S}, \mathcal{T})] \\ &+ \frac{1}{4} [2d_{\text{CMMD}}(\mathcal{S}|\mathbf{Z}, \mathcal{T}|\mathbf{Z})d_{\text{CMMD}}(\mathcal{S}, \mathcal{S}|\mathbf{Z}) + 2d_{\text{CMMD}}(\mathcal{S}|\mathbf{Z}, \mathcal{T}|\mathbf{Z})d_{\text{CMMD}}(\mathcal{T}, \mathcal{T}|\mathbf{Z}) + 2d_{\text{CMMD}}(\mathcal{S}|\mathbf{Z}, \mathcal{T}|\mathbf{Z})d_{\text{MMD}}(\mathcal{S}, \mathcal{T})] \\ &+ \frac{1}{4} [2d_{\text{CMMD}}(\mathcal{S}, \mathcal{S}|\mathbf{Z})d_{\text{CMMD}}(\mathcal{T}, \mathcal{T}|\mathbf{Z}) + 2d_{\text{CMMD}}(\mathcal{S}, \mathcal{S}|\mathbf{Z})d_{\text{MMD}}(\mathcal{S}, \mathcal{T}) + 2d_{\text{CMMD}}(\mathcal{T}, \mathcal{T}|\mathbf{Z})d_{\text{MMD}}(\mathcal{S}, \mathcal{T})] \end{aligned} \quad (21)$$

Since $d_{\text{CMMD}}(\mathcal{S}, \mathcal{S}|\mathbf{Z})$ and $d_{\text{CMMD}}(\mathcal{T}, \mathcal{T}|\mathbf{Z})$ measure the internal closeness of source \mathcal{S} and target domain \mathcal{T} , respectively; $d_{\text{CMMD}}(\mathcal{S}|\mathbf{Z}, \mathcal{T}|\mathbf{Z})$ and $d_{\text{MMD}}(\mathcal{S}, \mathcal{T})$ are both utilized to measure the closeness between source domain \mathcal{S} and target domain \mathcal{T} , the mixed MMD is invalid in domain adversarial learning, that is,

$$\begin{aligned} d_{\text{CMMD}}(\mathcal{S}|\mathbf{Z}, \mathcal{T}|\mathbf{Z})d_{\text{CMMD}}(\mathcal{S}, \mathcal{S}|\mathbf{Z}) &= 0 \\ d_{\text{CMMD}}(\mathcal{S}|\mathbf{Z}, \mathcal{T}|\mathbf{Z})d_{\text{CMMD}}(\mathcal{T}, \mathcal{T}|\mathbf{Z}) &= 0 \\ d_{\text{CMMD}}(\mathcal{S}, \mathcal{S}|\mathbf{Z})d_{\text{CMMD}}(\mathcal{T}, \mathcal{T}|\mathbf{Z}) &= 0 \\ d_{\text{CMMD}}(\mathcal{S}, \mathcal{S}|\mathbf{Z})d_{\text{MMD}}(\mathcal{S}, \mathcal{T}) &= 0 \\ d_{\text{CMMD}}(\mathcal{T}, \mathcal{T}|\mathbf{Z})d_{\text{MMD}}(\mathcal{S}, \mathcal{T}) &= 0. \end{aligned} \quad (22)$$

Therefore, the $d_{\text{CMMD}}^2(\mathcal{S}|\mathbf{Z}, \mathcal{T}|\mathbf{Z})$ satisfies

$$\begin{aligned} & d_{\text{CMMD}}^2(\mathcal{S}|\mathbf{Z}, \mathcal{T}|\mathbf{Z}) \\ & \leq \frac{1}{4} [d_{\text{CMMD}}^2(\mathcal{S}|\mathbf{Z}, \mathcal{T}|\mathbf{Z}) + d_{\text{CMMD}}^2(\mathcal{S}, \mathcal{S}|\mathbf{Z}) + d_{\text{CMMD}}^2(\mathcal{T}, \mathcal{T}|\mathbf{Z}) + d_{\text{MMD}}^2(\mathcal{S}, \mathcal{T}) + 2d_{\text{CMMD}}(\mathcal{T}, \mathcal{T}|\mathbf{Z})d_{\text{MMD}}(\mathcal{S}, \mathcal{T})] \end{aligned}$$

□

Corollary 1. In domain adversarial learning, the MMD can be transformed into a more tractable form from the perspective of loss function [33], that is,

$$\begin{aligned}
 & d_{\text{CMMD}}^2(\mathcal{S}|\mathbf{Z}, \mathcal{T}|\mathbf{Z}) \\
 & \Rightarrow \mathcal{L}(\mathcal{D}_S, \mathcal{D}_T, \mathcal{D}_{S|\mathbf{Z}}, \mathcal{D}_{T|\mathbf{Z}}; \mathcal{G}_S, \mathcal{G}_T) \\
 & = \mathcal{L}_1(\mathcal{D}_S, \mathcal{D}_T; \mathcal{G}_S, \mathcal{G}_T) + \mathcal{L}_2(\mathcal{D}_{S|\mathbf{Z}}, \mathcal{D}_{T|\mathbf{Z}}; \mathcal{G}_S, \mathcal{G}_T) \\
 & + \mathcal{L}_3(\mathcal{D}_S, \mathcal{D}_{S|\mathbf{Z}}; \mathcal{G}_S) + \mathcal{L}_4(\mathcal{D}_T, \mathcal{D}_{T|\mathbf{Z}}; \mathcal{G}_T) \\
 & + \mathcal{L}_1(\mathcal{D}_S, \mathcal{D}_T; \mathcal{G}_S, \mathcal{G}_T)^{\frac{1}{2}} \mathcal{L}_2(\mathcal{D}_{S|\mathbf{Z}}, \mathcal{D}_{T|\mathbf{Z}}; \mathcal{G}_S, \mathcal{G}_T)^{\frac{1}{2}}
 \end{aligned}$$

where $\mathcal{D}_S = \{\mathcal{S}, \hat{\mathcal{S}}\}$, $\mathcal{D}_T = \{\mathcal{T}, \hat{\mathcal{T}}\}$, $\mathcal{D}_{S|\mathbf{Z}} = \{\mathcal{S}, \hat{\mathcal{S}}\}_{|\mathbf{Z}}$ and $\mathcal{D}_{T|\mathbf{Z}} = \{\mathcal{T}, \hat{\mathcal{T}}\}_{|\mathbf{Z}}$, which $\hat{\mathcal{S}}$ and $\hat{\mathcal{T}}$ denote the generated source and target domains by sequence generators of source domain \mathcal{G}_S and target domain \mathcal{G}_T .

$$\begin{cases}
 \mathcal{L}_1 = \beta_1 \left\| \frac{1}{|\mathcal{D}_S|} \sum_{\mathbf{X} \in \mathcal{D}_S} \mathbf{X} - \frac{1}{|\mathcal{D}_T|} \sum_{\mathbf{X} \in \mathcal{D}_T} \mathbf{X} \right\|_2^2 \\
 \mathcal{L}_2 = \beta_2 \left\| \frac{1}{|\mathcal{D}_S|} \sum_{\mathbf{a} \in \mathbf{Z}} \sum_{\mathbf{X} \in \mathcal{D}_{S|\mathbf{Z}}} \mathbf{R}_{\mathbf{a}} - \frac{1}{|\mathcal{D}_T|} \sum_{\mathbf{a} \in \mathbf{Z}} \sum_{\mathbf{X} \in \mathcal{D}_{T|\mathbf{Z}}} \mathbf{R}_{\mathbf{a}} \right\|_2^2 \\
 \mathcal{L}_3 = \beta_3 \left\| \frac{1}{|\mathcal{D}_S|} \sum_{\mathbf{X} \in \mathcal{D}_S} \mathbf{X} - \frac{1}{|\mathcal{D}_{S|\mathbf{Z}}|} \sum_{\mathbf{a} \in \mathbf{Z}} \sum_{\mathbf{X} \in \mathcal{D}_{S|\mathbf{Z}}} \mathbf{R}_{\mathbf{a}} \right\|_2^2 \\
 \mathcal{L}_4 = \beta_4 \left\| \frac{1}{|\mathcal{D}_T|} \sum_{\mathbf{X} \in \mathcal{D}_T} \mathbf{X} - \frac{1}{|\mathcal{D}_{T|\mathbf{Z}}|} \sum_{\mathbf{a} \in \mathbf{Z}} \sum_{\mathbf{X} \in \mathcal{D}_{T|\mathbf{Z}}} \mathbf{R}_{\mathbf{a}} \right\|_2^2
 \end{cases}$$

where $\mathbf{R}_{\mathbf{a}} := \alpha(\mathbf{a}, \mathbf{k})\mathbf{X}$, \mathbf{k} denote the keys in transfer learning, $|\cdot|$ is the cardinality function, and the constants β are the balance parameters.

Proof. In domain adversarial learning, the MMD can be transformed into a more tractable form by computing the distance between source and target domain [33], that is,

$$d_{\text{MMD}}^2(\mathcal{S}, \mathcal{T}) \Rightarrow \mathcal{L}(\mathcal{S}, \mathcal{T}) = \left\| \frac{1}{|\mathcal{S}|} \sum_{\mathbf{X} \in \mathcal{S}} \mathbf{X} - \frac{1}{|\mathcal{T}|} \sum_{\mathbf{X} \in \mathcal{T}} \mathbf{X} \right\|_2^2 \quad (23)$$

Thus the independent loss functions of our proposed CDA can be formulized by utilizing Eq.(8), shown as

$$\begin{aligned}
 d_{\text{MMD}}^2(\mathcal{S}, \mathcal{T}) & \Rightarrow \mathcal{L}_1(\mathcal{D}_S, \mathcal{D}_T; \mathcal{G}_S, \mathcal{G}_T) = \left\| \frac{1}{|\mathcal{D}_S|} \sum_{\mathbf{X} \in \mathcal{D}_S} \mathbf{X} - \frac{1}{|\mathcal{D}_T|} \sum_{\mathbf{X} \in \mathcal{D}_T} \mathbf{X} \right\|_2^2 \\
 d_{\text{CMMD}}^2(\mathcal{S}|\mathbf{Z}, \mathcal{T}|\mathbf{Z}) & \Rightarrow \mathcal{L}_2(\mathcal{D}_{S|\mathbf{Z}}, \mathcal{D}_{T|\mathbf{Z}}; \mathcal{G}_S, \mathcal{G}_T) = \left\| \frac{1}{|\mathcal{D}_S|} \sum_{\mathbf{a} \in \mathbf{Z}} \sum_{\mathbf{X} \in \mathcal{D}_{S|\mathbf{Z}}} \mathbf{R}_{\mathbf{a}} - \frac{1}{|\mathcal{D}_T|} \sum_{\mathbf{a} \in \mathbf{Z}} \sum_{\mathbf{X} \in \mathcal{D}_{T|\mathbf{Z}}} \mathbf{R}_{\mathbf{a}} \right\|_2^2 \\
 d_{\text{CMMD}}^2(\mathcal{S}, \mathcal{S}|\mathbf{Z}) & \Rightarrow \mathcal{L}_3(\mathcal{D}_S, \mathcal{D}_{S|\mathbf{Z}}; \mathcal{G}_S) = \left\| \frac{1}{|\mathcal{D}_S|} \sum_{\mathbf{X} \in \mathcal{D}_S} \mathbf{X} - \frac{1}{|\mathcal{D}_{S|\mathbf{Z}}|} \sum_{\mathbf{a} \in \mathbf{Z}} \sum_{\mathbf{X} \in \mathcal{D}_{S|\mathbf{Z}}} \mathbf{R}_{\mathbf{a}} \right\|_2^2 \\
 d_{\text{CMMD}}^2(\mathcal{T}, \mathcal{T}|\mathbf{Z}) & \Rightarrow \mathcal{L}_4(\mathcal{D}_T, \mathcal{D}_{T|\mathbf{Z}}; \mathcal{G}_T) = \left\| \frac{1}{|\mathcal{D}_T|} \sum_{\mathbf{X} \in \mathcal{D}_T} \mathbf{X} - \frac{1}{|\mathcal{D}_{T|\mathbf{Z}}|} \sum_{\mathbf{a} \in \mathbf{Z}} \sum_{\mathbf{X} \in \mathcal{D}_{T|\mathbf{Z}}} \mathbf{R}_{\mathbf{a}} \right\|_2^2
 \end{aligned} \quad (24)$$

Therefore, we have for Eq.(21)

$$\begin{aligned}
& d_{\text{CMMD}}^2(\mathcal{S}|\mathbf{Z}, \mathcal{T}|\mathbf{Z}) \\
& \leq \frac{1}{4} \left\| \frac{1}{|\mathcal{D}_S|} \sum_{\mathbf{X} \in \mathcal{D}_S} \mathbf{X} - \frac{1}{|\mathcal{D}_T|} \sum_{\mathbf{X} \in \mathcal{D}_T} \mathbf{X} \right\|_2^2 + \frac{1}{4} \left\| \frac{1}{|\mathcal{D}_S|} \sum_{\mathbf{a} \in \mathbf{Z}} \sum_{\mathbf{X} \in \mathcal{D}_{S|\mathbf{Z}}} \mathbf{R}_a - \frac{1}{|\mathcal{D}_T|} \sum_{\mathbf{a} \in \mathbf{Z}} \sum_{\mathbf{X} \in \mathcal{D}_{T|\mathbf{Z}}} \mathbf{R}_a \right\|_2^2 \\
& + \frac{1}{4} \left\| \frac{1}{|\mathcal{D}_S|} \sum_{\mathbf{X} \in \mathcal{D}_S} \mathbf{X} - \frac{1}{|\mathcal{D}_{S|\mathbf{Z}}|} \sum_{\mathbf{a} \in \mathbf{Z}} \sum_{\mathbf{X} \in \mathcal{D}_{S|\mathbf{Z}}} \mathbf{R}_a \right\|_2^2 + \frac{1}{4} \left\| \frac{1}{|\mathcal{D}_T|} \sum_{\mathbf{X} \in \mathcal{D}_T} \mathbf{X} - \frac{1}{|\mathcal{D}_{T|\mathbf{Z}}|} \sum_{\mathbf{a} \in \mathbf{Z}} \sum_{\mathbf{X} \in \mathcal{D}_{T|\mathbf{Z}}} \mathbf{R}_a \right\|_2^2 \\
& + \frac{1}{2} \left\| \frac{1}{|\mathcal{D}_S|} \sum_{\mathbf{X} \in \mathcal{D}_S} \mathbf{X} - \frac{1}{|\mathcal{D}_T|} \sum_{\mathbf{X} \in \mathcal{D}_T} \mathbf{X} \right\|_2 \cdot \left\| \frac{1}{|\mathcal{D}_S|} \sum_{\mathbf{a} \in \mathbf{Z}} \sum_{\mathbf{X} \in \mathcal{D}_{S|\mathbf{Z}}} \mathbf{R}_a - \frac{1}{|\mathcal{D}_T|} \sum_{\mathbf{a} \in \mathbf{Z}} \sum_{\mathbf{X} \in \mathcal{D}_{T|\mathbf{Z}}} \mathbf{R}_a \right\|_2
\end{aligned} \tag{25}$$

Hence, by utilizing the Eq.(8) the unified loss function of domain classification $\mathcal{L}(\mathcal{D}_S, \mathcal{D}_T, \mathcal{D}_{S|\mathbf{Z}}, \mathcal{D}_{T|\mathbf{Z}}; \mathcal{G}_S, \mathcal{G}_T)$ can be derived as

$$\begin{aligned}
& \mathcal{L}(\mathcal{D}_S, \mathcal{D}_T, \mathcal{D}_{S|\mathbf{Z}}, \mathcal{D}_{T|\mathbf{Z}}; \mathcal{G}_S, \mathcal{G}_T) \\
& = \beta_1 \left\| \frac{1}{|\mathcal{D}_S|} \sum_{\mathbf{X} \in \mathcal{D}_S} \mathbf{X} - \frac{1}{|\mathcal{D}_T|} \sum_{\mathbf{X} \in \mathcal{D}_T} \mathbf{X} \right\|_2^2 + \beta_2 \left\| \frac{1}{|\mathcal{D}_{S|\mathbf{Z}}|} \sum_{\mathbf{a} \in \mathbf{Z}} \sum_{\mathbf{X} \in \mathcal{D}_{S|\mathbf{Z}}} \mathbf{R}_a - \frac{1}{|\mathcal{D}_{T|\mathbf{Z}}|} \sum_{\mathbf{a} \in \mathbf{Z}} \sum_{\mathbf{X} \in \mathcal{D}_{T|\mathbf{Z}}} \mathbf{R}_a \right\|_2^2 \\
& + \beta_3 \left\| \frac{1}{|\mathcal{D}_S|} \sum_{\mathbf{X} \in \mathcal{D}_S} \mathbf{X} - \frac{1}{|\mathcal{D}_{S|\mathbf{Z}}|} \sum_{\mathbf{a} \in \mathbf{Z}} \sum_{\mathbf{X} \in \mathcal{D}_{S|\mathbf{Z}}} \mathbf{R}_a \right\|_2^2 + \beta_4 \left\| \frac{1}{|\mathcal{D}_T|} \sum_{\mathbf{X} \in \mathcal{D}_T} \mathbf{X} - \frac{1}{|\mathcal{D}_{T|\mathbf{Z}}|} \sum_{\mathbf{a} \in \mathbf{Z}} \sum_{\mathbf{X} \in \mathcal{D}_{T|\mathbf{Z}}} \mathbf{R}_a \right\|_2^2 \\
& + \gamma \left\| \frac{1}{|\mathcal{D}_S|} \sum_{\mathbf{X} \in \mathcal{D}_S} \mathbf{X} - \frac{1}{|\mathcal{D}_T|} \sum_{\mathbf{X} \in \mathcal{D}_T} \mathbf{X} \right\|_2 \cdot \left\| \frac{1}{|\mathcal{D}_{S|\mathbf{Z}}|} \sum_{\mathbf{a} \in \mathbf{Z}} \sum_{\mathbf{X} \in \mathcal{D}_{S|\mathbf{Z}}} \mathbf{R}_a - \frac{1}{|\mathcal{D}_{T|\mathbf{Z}}|} \sum_{\mathbf{a} \in \mathbf{Z}} \sum_{\mathbf{X} \in \mathcal{D}_{T|\mathbf{Z}}} \mathbf{R}_a \right\|_2
\end{aligned} \tag{26}$$

where $\mathbf{R}_a := \alpha(\mathbf{a}, \mathbf{k})\mathbf{X}$, which \mathbf{k} denote the keys in transfer learning, the constants β and γ are the balance parameters, and $|\cdot|$ is the cardinality function. \square

